Matching and Biasing Networks

As pointed out in Chapter 2, to achieve maximum power transfer, we need to match the impedance of the load to that of the source. Usually this is accomplished by incorporating additional passive networks connected in-between source and load. These networks are generically referred to as matching networks. However, their functionality is not simply limited to matching source and load impedances for optimal power flow. In fact, for many practical circuits matching networks are not only designed to meet the requirement of minimum power loss but are also based on additional constraints, such as minimizing the noise influence, maximizing power handling capabilities, and linearizing the frequency response. In a more general context, the purpose of a matching network can be defined as a transformation to convert a given impedance value to another, more suitable value.

In this chapter we restrict our coverage to the techniques of performing impedance transformation using passive matching networks. The emphasis is to ensure minimum reflections between source and load. All remaining considerations, such as noise figure and linearity, are left for discussions in Chapter 9.

We commence with a study of networks based on discrete components. These networks are easy to analyze and can be used up to frequencies in the low GHz range. Next, we continue with the analysis and design of matching networks using distributed elements, such as strip lines and stub sections. These networks are more suitable for operational frequencies exceeding 1 GHz, or for cases where vertical circuit dimensions are of importance, as required in RF integrated circuit designs.

To simplify our treatment and to gain clarity in the design methodology, the Smith Chart will be utilized extensively throughout as a primary design tool.

8.1 Impedance Matching Using Discrete Components

8.1.1 Two-Component Matching Networks

In a generic sense our engineering efforts primarily strive for two main goals: first, to meet system specifications, and second, to find the most inexpensive and reliable way to accomplish this first task. The cheapest and most reliable matching networks are usually those that contain the least number of components.

The topic of this section is to analyze and design the simplest possible type of matching networks: so-called **two-component networks**, also known as **L-sections** due to their element arrangement. These networks use two reactive components to transform the load impedance (Z_L) to the desired input impedance (Z_{in}). In conjunction with the load and source impedances, the components are alternatively connected in series and shunt configuration, as shown in Figure 8-1, which depicts eight possible arrangements of capacitors and inductors.

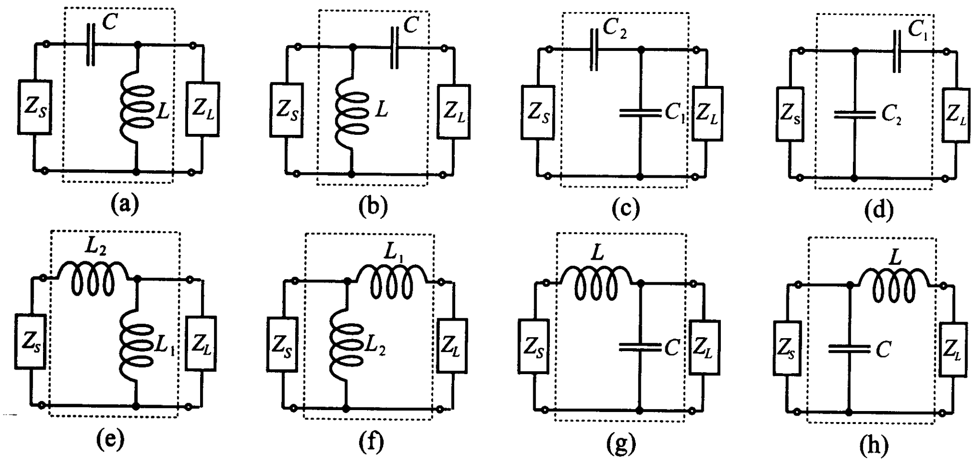

Figure 8-1 Eight possible configurations of the discrete two-component matching networks.

In designing a matching network we have two broad approaches at our disposal:

1. To derive the values of the elements analytically
2. To rely on the Smith Chart as a graphical design tool

The first approach yields very precise results and is suitable for computer synthesis. Alternatively, the second approach is more intuitive, easier to verify, and faster for an initial design, since it does not require complicated computations. The example below details the use of the analytical approach to design a particular L-section matching network.

Example 8-1: Analytical approach to the design of an L-section matching network

The output impedance of a transmitter operating at a frequency of 2 GHz is $Z_T = (150 + j75)\Omega$. Design an L-section matching network, as shown in Figure 8-2, such that maximum power is delivered to the antenna whose input impedance is $Z_A = (75 + j15)\Omega$.

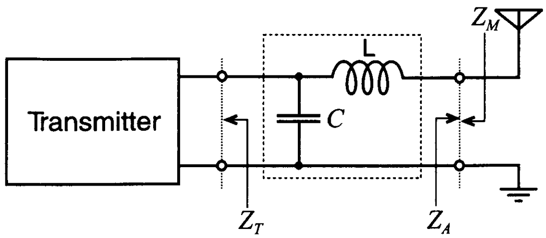

Figure 8-2 Transmitter to antenna matching circuit design.

Solution: The condition of maximum power transfer from the source to the load requires the source impedance to be equal to the complex conjugate of the load impedance. In our case this implies that the output impedance Z_M of the matching network has to be equal to the complex conjugate of Z_A [i.e., $Z_M = Z_A^* = (75 - j15)\Omega$].

The impedance Z_M can be computed as a series connection of an inductor L and a parallel combination of C and Z_T:

$$Z_M = \frac{1}{Z_T^{-1} + jB_C} + jX_L = Z_A^* \tag{8.1}$$

where $B_C = \omega C$ is the susceptance of the capacitor and $X_L = \omega L$ is the reactance of the inductor. Expressing transmitter and antenna impedances in terms of their real and imaginary parts (i.e., $Z_T = R_T + jX_T$ and $Z_A = R_A + jX_A$), we can rewrite (8.1) as

$$\frac{R_T + jX_T}{1 + jB_C(R_T + jX_T)} + jX_L = R_A - jX_A \tag{8.2}$$

Separating real and imaginary parts in (8.2), a system of two equations is found:

$$R_T = R_A(1 - B_C X_T) + (X_A + X_L)B_C R_T \tag{8.3a}$$

$$X_T = R_T R_A B_C - (1 - B_C X_T)(X_A + X_L) \tag{8.3b}$$

Solving (8.3a) for X_L and substituting into (8.3b) results in a quadratic equation for B_C whose solution is

$$B_C = \frac{X_T \pm \sqrt{\frac{R_T}{R_A}(R_T^2 + X_T^2) - R_T^2}}{R_T^2 + X_T^2} \tag{8.4}$$

Since $R_T > R_A$, the argument of the square root is positive and greater than X_T^2. Therefore, to ensure a positive B_C we must choose the "plus" sign in (8.4). Substituting (8.4) into (8.3a) yields X_L as

$$X_L = \frac{1}{B_C} - \frac{R_A(1 - B_C X_T)}{B_C R_T} - X_A \tag{8.5}$$

Inserting numerical values into (8.4) and (8.5), we find

$$B_C = 9.2 \text{ mS} \Rightarrow C = B_C/\omega = 0.73 \text{ pF}$$

$$X_L = 76.9\ \Omega \Rightarrow L = X_L/\omega = 6.1 \text{ nH}$$

This example shows the analytical approach of designing an L-section matching network by solving a quadratic equation for C and then a linear equation for L. The process is tedious but can be easily implemented on a mathematical spreadsheet.

As we may anticipate from Example 8-1, the analytical approach of designing matching networks can become very complicated and computationally intensive even for simple L-sections. Instead of the preceding method, we can use the Smith Chart for rapid and relatively precise designs of the matching circuits. The appeal of this approach is that its complexity remains almost the same independent of the number of components in the network. Moreover, by observing the impedance transformation on the Smith Chart we obtain a "feel" of how the individual circuit elements contribute to achieving a particular matching condition. Any errors in component selection and value assignment are observed immediately and the design engineer can directly intervene. With the help of a personal computer, this process is carried out in real time. That is, the parameter choice (L or C) and its value assignment can be instantaneously displayed as part of the Smith Chart on the computer screen.

The effect of connecting a single reactive component (either capacitor or inductor) to a complex load is described in considerable detail in Section 3.4. Here we just point out the following:

- The addition of a reactance connected in series with a complex impedance results in motion along a constant-resistance circle in the combined Smith Chart
- A shunt connection produces motion along a constant-conductance circle.

This is indicated in Figure 8-3 for the combined *ZY* Smith Chart. Concerning the direction of the rotation, the general rule of thumb is that whenever an inductor is involved, we rotate in the direction that moves the impedance into the upper half of the Smith Chart. In contrast, a capacitance results in the movement toward the lower half.

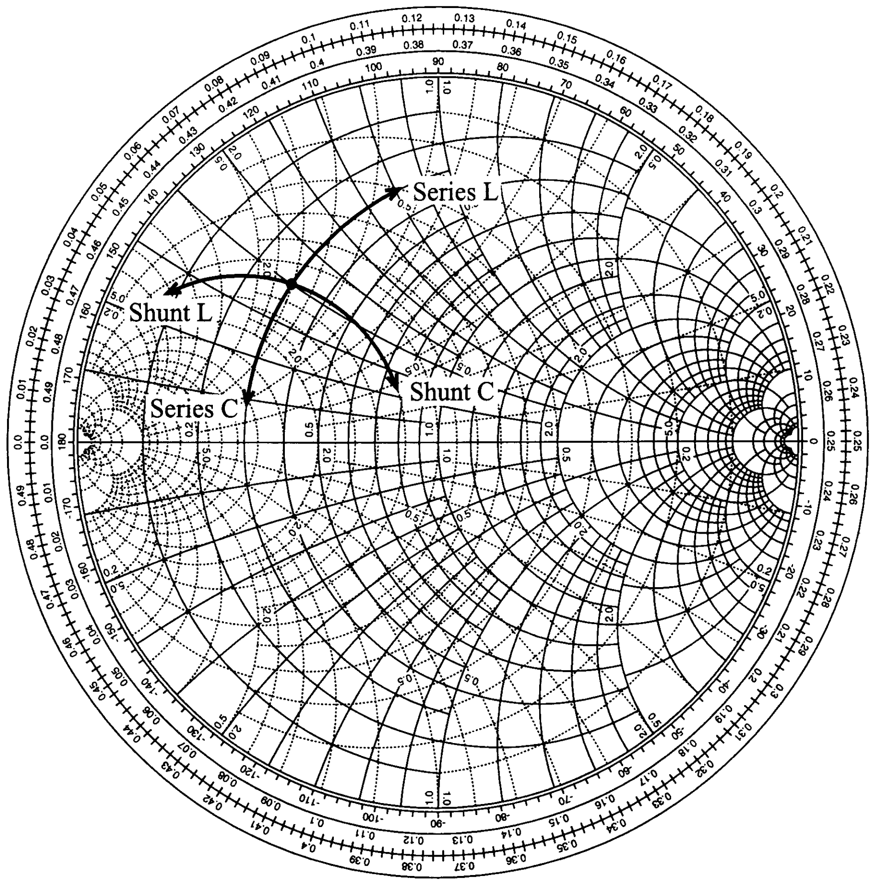

Figure 8-3 Impedance effect of series and shunt connections of *L* and *C* to a complex load in the Smith Chart.

Having established the effect of connecting a single component to the load, we can now develop suitable two-component matching networks that perform the transformation from any load impedance to any specified input impedance. In general, designing an L-type matching network, or for that matter any passive network, in the *ZY* Smith Chart consists of moving along either constant resistance or constant conductance circles.

In the following example we illustrate this graphical design technique as an alternative to the analytical approach discussed in Example 8-1. Most modern CAD programs allow us to conduct this graphical approach interactively on the computer screen. In fact, simulation packages such as MMICAD directly permit the placement of components with the corresponding impedance behavior displayed on the Smith Chart.

RF&MW→

Example 8-2: Graphical approach to the design of the L-section matching network

Design the L-type reactive matching network discussed in Example 8-1 by using the Smith Chart as a graphical design tool.

Solution: The first step is to compute normalized transmitter and antenna impedances. Since no characteristic impedance Z_0 is given, we arbitrarily select $Z_0 = 75\ \Omega$. Therefore, the normalized transmitter and antenna impedances are $z_T = Z_T/Z_0 = 2 + j1$ and $z_A = Z_A/Z_0 = 1 + j0.2$, respectively. Since the first component connected to the transmitter is a shunt capacitor, the total impedance of this parallel combination is positioned somewhere on the circle of constant conductance that passes through the point z_T in the combined Smith Chart (see Figure 8-4).

Next, an inductor is added in series with the parallel combination of transmitter z_T and capacitor; the resulting impedance will move along the circle of constant resistance. For maximum power gain we require an output impedance of the matching network connected to the transmitter to be equal to the complex conjugate of the antenna impedance. This circle has to pass through $z_M = z_A^* = 1 - j0.2$, as shown in Figure 8-4.

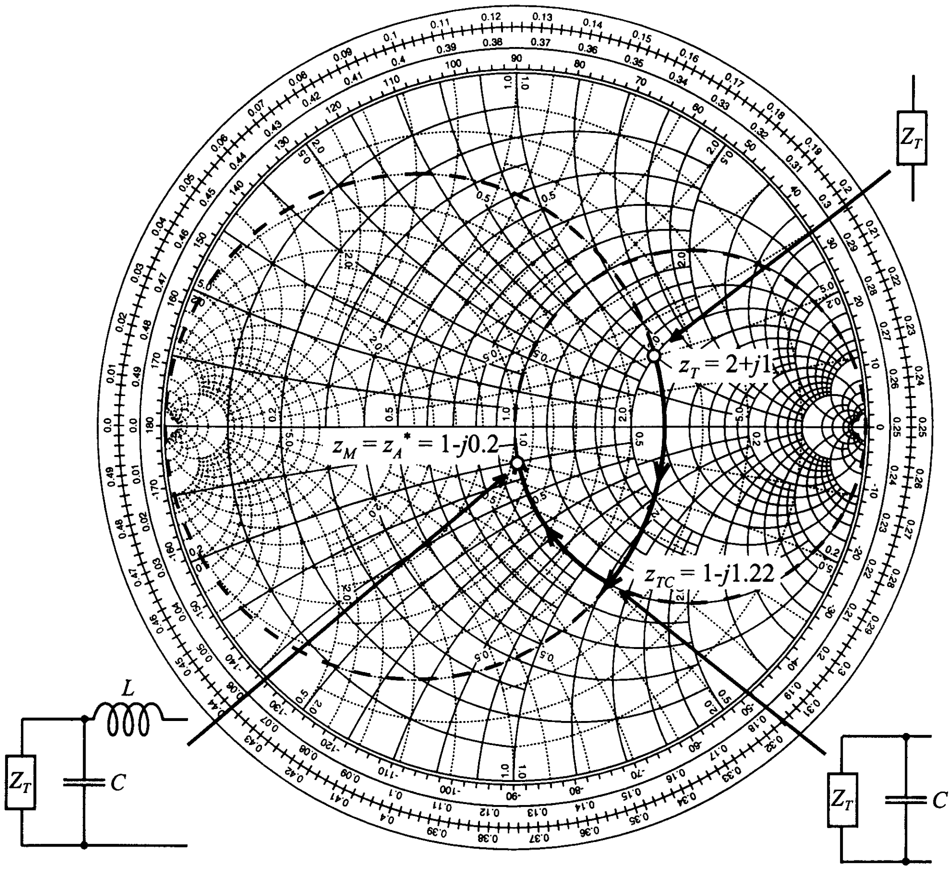

Figure 8-4 Design of the two-element matching network as part of the *ZY* Smith Chart.

The intersection of two circles in the Smith Chart determines the normalized impedance formed by the shunt connection of transmitter and capacitor. Reading from the Smith Chart, we find that this impedance is approximately $z_{TC} = 1 - j1.22$ with the corresponding admittance of $y_{TC} = 0.4 + j0.49$. Therefore, the normalized susceptance of the shunt capacitor is $jb_C = y_{TC} - y_T = j0.69$ and the normalized reactance of the inductor is $jx_L = z_A - z_{TC} = j1.02$. Finally, the actual values for the inductor and capacitor are

$$L = (x_L Z_0)/\omega = 6.09 \text{ nH}$$

$$C = b_C/(\omega Z_0) = 0.73 \text{ pF}$$

This example presents a simple and yet precise graphical approach to design L-section matching networks. The method can be readily extended to more complicated systems.

The design procedure described in Example 8-2 can be applied to any L-section matching network shown in Figure 8-1. The generic solution procedure for optimal power transfer includes the following six steps:

1. Find the normalized source and load impedances.
2. In the Smith Chart plot circles of constant resistance and conductance that pass through the point denoting the source impedance.
3. Plot circles of constant resistance and conductance that pass through the point of the *complex conjugate* of the load impedance.
4. Identify the intersection points between the circles in steps 2 and 3. The number of intersection points determines the number of possible L-section matching networks.
5. Find the values of the normalized reactances and susceptances of the inductors and capacitors by tracing a path along the circles from the source impedance to the intersection point and then to the complex conjugate of the load impedance.
6. Determine the actual values of inductors and capacitors for a given frequency.

In the preceding steps it is not necessary to move from the source to the complex conjugate load impedance. As a matter of fact, we can transform the load to the complex conjugate source impedance. The following example illustrates the first approach, whereas Section 8.1.2 discusses the second method.

Example 8-3: Design of general two-component matching networks

Using the Smith Chart, design all possible configurations of discrete two-element matching networks that match the source impedance $Z_S = (50 + j25)\Omega$ to the load $Z_L = (25 - j50)\Omega$. Assume a characteristic impedance of $Z_0 = 50\ \Omega$ and an operating frequency of $f = 2$ GHz.

Solution: We follow the six steps listed previously.

1. The normalized load and source impedances are:

$$z_S = Z_S/Z_0 = 1 + j0.5 \text{ or } y_S = 0.8 - j0.4$$

$$z_L = Z_L/Z_0 = 0.5 - j1 \text{ or } y_L = 3 + j0.8$$

2. We plot circles of constant resistance and constant conductance that pass through the points of the normalized source impedance (dashed line circles in Figure 8-5), and

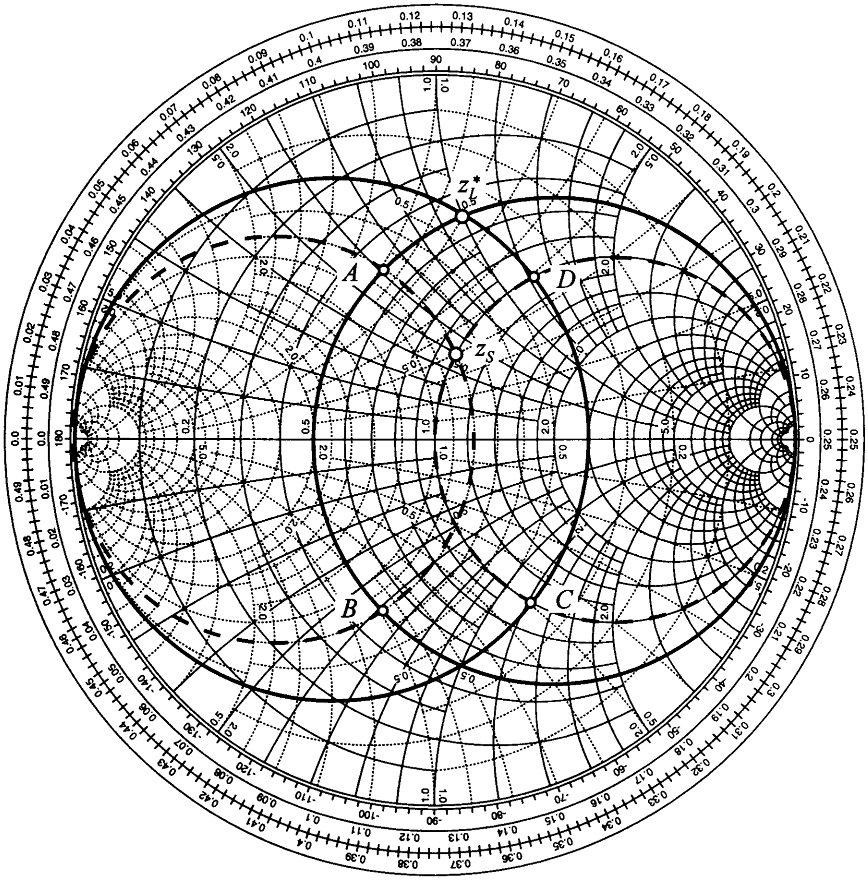

Figure 8-5 Design of a matching network using the Smith Chart

3. Complex conjugate of the load impedance (solid line circles in Figure 8-5).

4. These circles intersect in four points denoted as A, B, C, and D, with the normalized impedances and admittances being as follows:

$$z_A = 0.5 + j0.6, \quad y_A = 0.8 - j1$$
$$z_B = 0.5 - j0.6, \quad y_B = 0.8 + j1$$
$$z_C = 1 - j1.2, \quad y_C = 3 + j0.5$$
$$z_D = 1 + j1.2, \quad y_D = 3 - j0.5$$

5. Since there are four intersection points, we expect four possible configurations of L-section matching networks. Indeed, if we move along the $z_S \to z_A \to z_L^*$ path we see that from point z_S to z_A the impedance is transformed along the circle of constant conductance indicating shunt connection. Moreover, we move toward the upper half of the Smith Chart (see Figure 8-3), which indicates that the first component connected to the source should be a shunt inductor. From points z_A to z_L^* the impedance is transformed along the circle of constant resistance, with movement toward the upper half of the chart indicating series connection of the inductance. Therefore, the $z_S \to z_A \to z_L^*$ path results in a "**shunt L, series L**" matching network, as shown in Figure 8-1(f). If the $z_S \to z_B \to z_L^*$ path is chosen, we obtain a "**shunt C, series L**" network [Figure 8-1(h)]. For $z_S \to z_C \to z_L^*$ the matching network is "**series C, shunt L**" [Figure 8-1(a)]. Finally, for the $z_S \to z_D \to z_L^*$ path, a matching network is constructed by a "**series L, shunt L**" combination, which is shown in Figure 8-1(e).
6. We finally have to find the actual component values for the matching networks identified in the previous step. If we direct our attention again to the $z_S \to z_A \to z_L^*$ path, we see that from the source impedance to the point z_A the normalized admittance of the circuit is changed by

$$jb_{L_2} = y_A - y_S = (0.8 - j1) - (0.8 - j0.4) = -j0.6$$

From here the value of the shunt inductor is:

$$L_2 = -\frac{Z_0}{b_{L_2}\omega} = 6.63nH$$

Transformation from point z_A to z_L^* is done by adding an inductor connected in series to the impedance z_A. Therefore,

$$jx_{L_1} = z_L^* - z_A = (0.5 + j1) - (0.5 + j0.6) = j0.4$$

and the value of this inductor is

$$L_1 = \frac{x_{L_1} Z_0}{\omega} = 1.59 \text{ nH}$$

The values of the components for the remaining three matching networks are found in the same way. The results are shown in Figure 8-6.

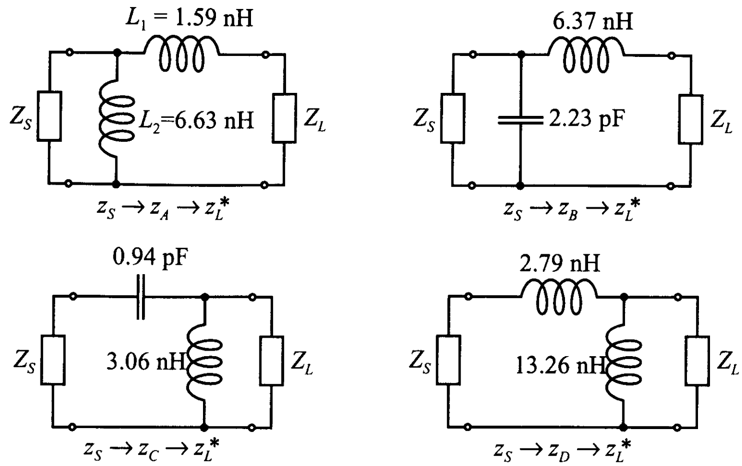

Figure 8-6 Matching networks for four different paths in the Smith Chart.

The Smith Chart allows us immediate observation whether or not a particular impedance transformation is capable of achieving the desired matching. Moreover, the total number of possible network connections can readily be seen.

8.1.2 Forbidden Regions, Frequency Response, and Quality Factor

Before continuing with the frequency analysis of L-type matching networks, let us first note that not every network topology depicted in Figure 8-1 can perform the required matching between arbitrary load and source impedances. For example, if the source is $Z_S = Z_0 = 50\ \Omega$ and if we use a matching network shown in Figure 8-1(h), then the addition of the capacitor in parallel with the source produces motion in clockwise direction away from the circle of constant resistance that passes through the origin. This implies that all load impedances that fall into the shaded region in Figure 8-7(a) cannot be matched to the 50 Ω source by this particular network.

Similar "forbidden regions" can be developed for all L-type matching network topologies depicted in Figure 8-1. Examples of such regions for several other networks

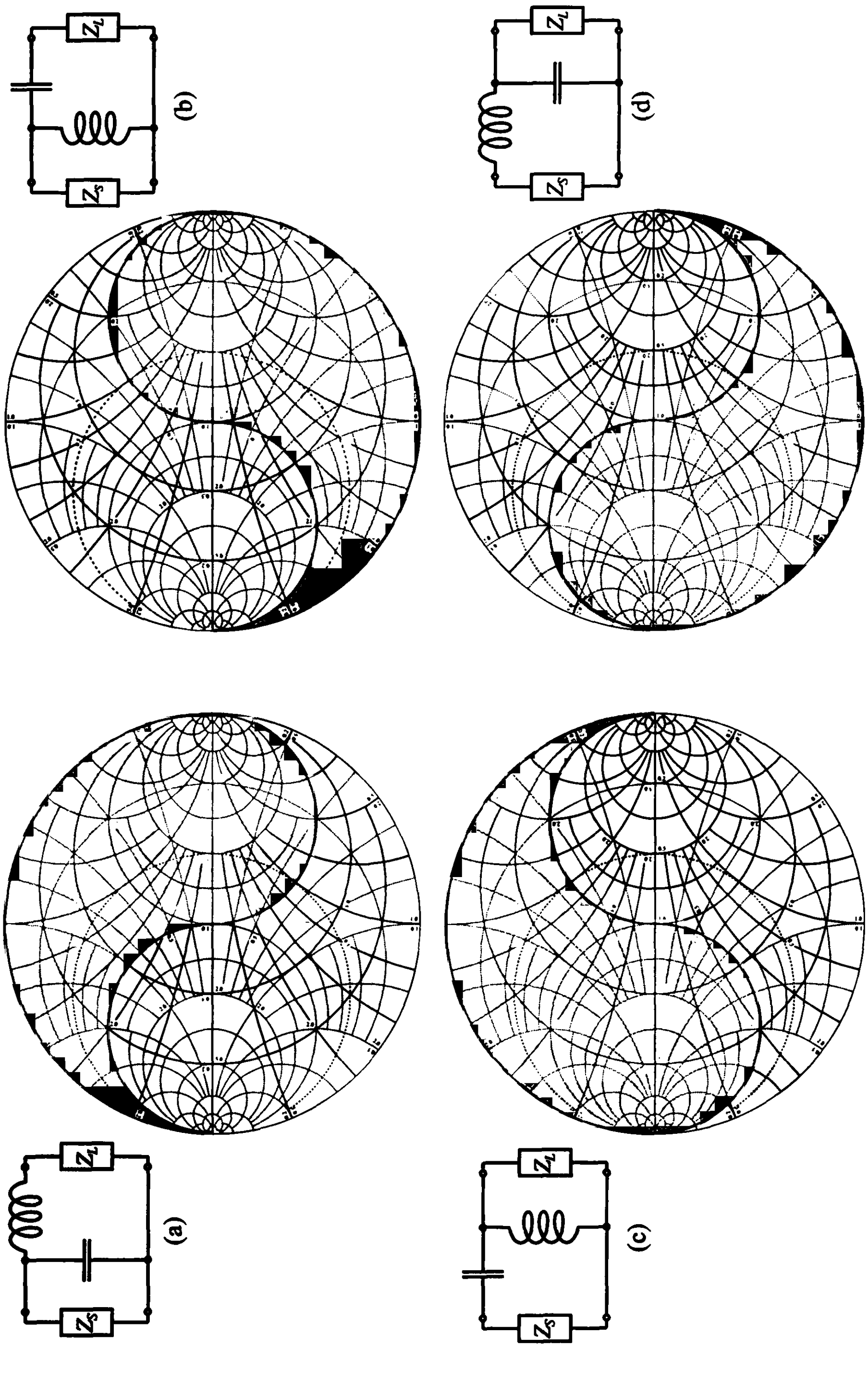

Figure 8-7 Forbidden regions for L-type matching networks with $Z_S = Z_0 = 50\ \Omega$.

based on a 50 Ω source impedance are shown in Figure 8-7. Here the shaded areas denote values of the load impedance that cannot be matched to the 50 Ω source. It is important to keep in mind that the forbidden regions in Figure 8-7 are applicable only when dealing with a $Z_S = Z_0 = 50\ \Omega$ source impedance. The regions take on totally different shapes for other source impedance values.

As explained in Example 8-3 and displayed in Figure 8-7, for any given load and input impedances there are at least two possible configurations of L-type networks that accomplish the required match. The question now is, what is the difference between these realizations and which network should ultimately be chosen?

Besides the obvious reasons for selecting one network over another (for instance, availability of components with required values), there are key technical considerations, including DC biasing, stability, and frequency response. In the remainder of this section we concentrate primarily on the frequency response and quality factor of the L-type matching networks, whereas DC biasing issues are covered later in Section 8.3. Stability is deferred to Chapter 9.

Since any L-type matching network consists of series and shunt combinations of capacitors and/or inductors, the frequency response of these networks can be classified as either low-pass, high-pass, or bandpass filters. To demonstrate such behavior, let us consider a matching network that transforms a complex load, consisting of resistance $R_L = 80\ \Omega$ connected in series with capacitor $C_L = 2.65\ \text{pF}$, into a 50 Ω input impedance. Let us further assume that the operational frequency for this circuit is $f_0 = 1$ GHz.

At 1 GHz the normalized load impedance is $z_L = 1.6 - j1.2$, and according to Figure 8-7 we can use either one of the matching networks shown in Figure 8-7(c) or Figure 8-7(d), following a similar design procedure as described in Example 8-2. However, because the source impedance z_S is real ($z_S = 50\ \Omega$) it is easier to transform from the load to the source impedance since $z_S^* = z_S = 50\ \Omega$. This is shown in Figure 8-8(a). The corresponding matching networks are shown in Figures 8-8(b) and 8-8(c).

The frequency responses of these two networks in terms of the input reflection coefficient $\Gamma_{\text{in}} = (Z_{\text{in}} - Z_S)/(Z_{\text{in}} + Z_S)$ and the transfer function $H = V_{\text{out}}/V_S$ (where the output voltage V_{out} is measured across the load resistance $R_L = 80\ \Omega$) are shown in Figures 8-9(a) and (b), respectively.

It is apparent from Figure 8-9 that both networks exhibit perfect matching only at a particular frequency $f_0 = 1$ GHz and begin to deviate quickly when moving away from f_0.

The previously developed matching networks can also be viewed as resonance circuits with f_0 being the resonance frequency. As discussed in Section 5.1.1, these

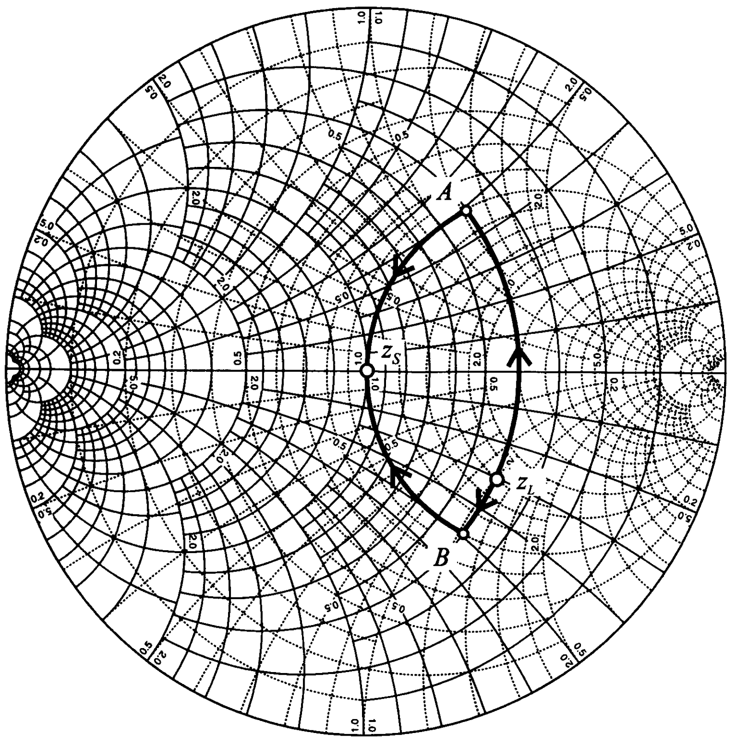

(a) Impedance transformations displayed in Smith Chart

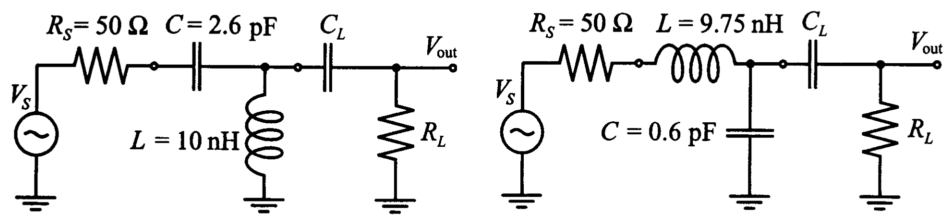

(b) (c)

Resulting matching networks

Figure 8-8 Two design realizations of an L-type matching network.

networks may be described by a loaded quality factor, Q_L, which is equal to the ratio of the resonance frequency f_0 over the 3 dB bandwidth BW

$$Q_L = \frac{f_0}{BW} \tag{8.6}$$

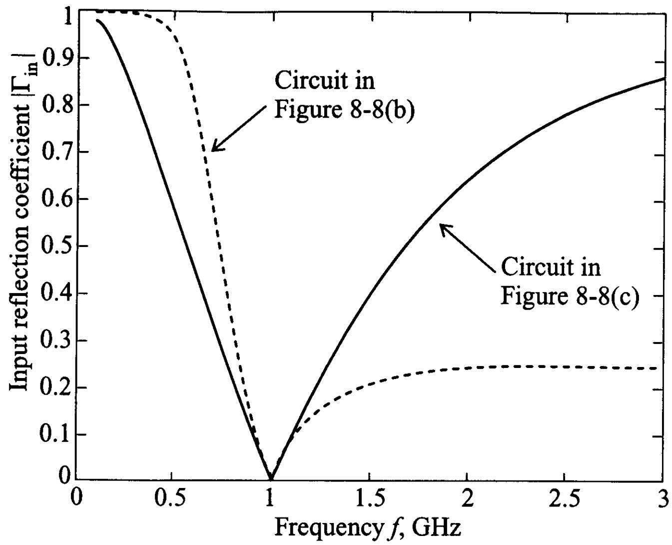

(a) Frequency response of input reflection coefficient

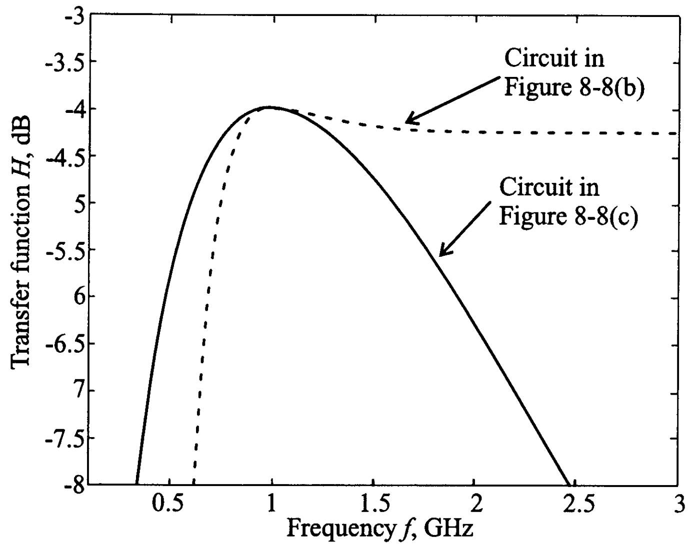

(b) Transfer function of the matching networks

Figure 8-9 Frequency response of the two matching network realizations.

where both f_0 and BW are expressed in Hz. The question now is how to find the bandwidth of the matching network. To answer this, we will exploit the similarity between the bell-shaped response of the matching network's transfer function near f_0 [see Figure 8-9(b)] and the frequency response of a bandpass filter.

For frequencies close to f_0 the matching network in Figure 8-8(c) can be redrawn as a bandpass filter with a loaded quality factor calculated based on (8.6). The equivalent bandpass filter is shown in Figure 8-10(a). The equivalent capacitance C_T in this circuit is obtained by replacing the series combination of R_L and C_L in Figure 8-8(c) with an equivalent parallel connection of R_{LP} and C_{LP} and then adding the capacitances C and C_{LP}: $C_T = C + C_{LP}$. The equivalent shunt inductance L_{LN} is obtained by first replacing the series connection of the voltage source V_S, resistance R_S, and inductance L with the Norton equivalent current source $I_N = V_S/(R_S + j\omega_0 L)$ connected to the parallel combination of conductance G_{SN} and inductance L_N, where the admittance is given as follows: $G_{SN} + (j\omega_0 L_N)^{-1} = (R_S + j\omega_0 L)^{-1}$. Next, the current source I_N and conductance G_{SN} are converted back into a Thévenin equivalent voltage source

$$V_T = I_N/G_{SN} = V_S\frac{R_S - j\omega_0 L}{R_S} = V_S(1 - j1.2255) \tag{8.7}$$

and series resistance

$$R_{ST} = G_{SN}^{-1} = \frac{R_S^2 + (\omega_0 L)^2}{R_S} \tag{8.8}$$

The resonance circuit in Figure 8-10 is loaded by the combined resistance $R_T = R_L \| R_{ST} = 62.54\ \Omega$. Thus, the loaded quality factor Q_L of the equivalent bandpass filter is given by

$$Q_L = \frac{f_0}{BW} = \omega_0 R_T C = \frac{R_T}{|X_C|} = 0.61 \tag{8.9}$$

It is immediately noticed that the maximum gain for the equivalent bandpass filter is higher than the gain of the original matching network. This is explained by the fact that for the matching network we measure the output voltage on the load R_L, while for the equivalent filter we measure the output voltage at the equivalent load resistance R_{LP}, which is connected in parallel with the capacitance C_T. Therefore, the conversion from V_b to V_{out} at the resonance frequency can be found through the voltage divider rule:

$$|V_{out}| = |V_b|\frac{R_L}{\left|R_L + \frac{1}{j\omega_0 C_L}\right|} = 0.7908|V_b|$$

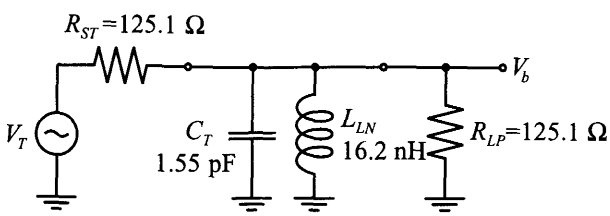

(a) Equivalent bandpass filter

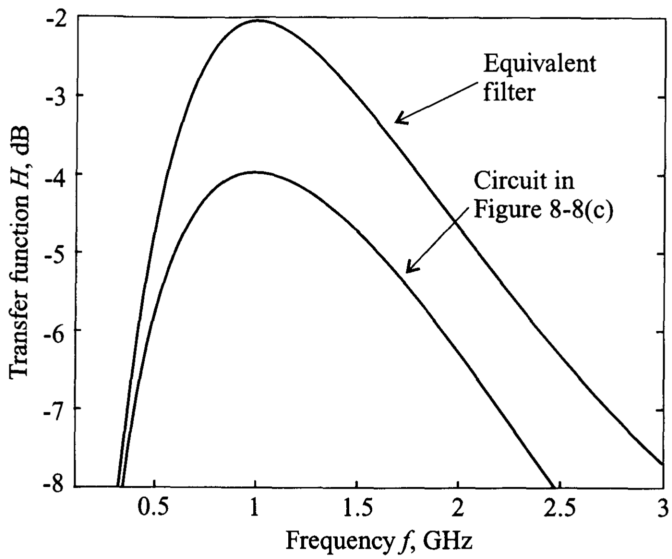

(b) Frequency response of the matching network compared to the equivalent filter response

Figure 8-10 Comparison of the frequency response of the L-type matching network and an equivalent bandpass filter.

which gives us

$$20\log\frac{|V_{\text{out}}|}{|V_S|} = -2.0382 + 20\log\frac{|V_b|}{|V_S|} = -3.9794 \text{ dB}$$

a result that agrees very well with Figure 8-9(b).

From the known Q_L we can directly find the bandwidth of the filter: $BW = f_0/Q_L = 1.63$ GHz. The frequency response in Figure 8-9(b) shows that the 3 dB point for $f < f_0$ occurs at $f_{\min} = 0.40$ GHz and for $f > f_0$ the 3 dB point corresponds to $f_{\max} = 2.19$ GHz. Thus, the bandwidth of the matching network is

$BW = f_{max} - f_{min} = 1.79\ \text{GHz}$, which again agrees reasonably well with the result obtained for the equivalent bandpass filter.

The equivalent bandpass filter analysis allows us to explain the bell-shaped response of the matching network in the neighborhood of f_0 and provides us with a good estimation of the bandwidth of the circuit. The only drawback to this approach is its complexity. It would be desirable to develop a simpler method of estimating the quality factor of the matching network without having first to develop an equivalent bandpass filter or even computing the frequency response of the network. This is accomplished through the use of a so-called **nodal quality factor** Q_n.

Let us go back to Figure 8-8(a), where we illustrate the impedance transformation as we move from one node of the circuit to another. We note that at each node of the matching network the impedance can be expressed in terms of an equivalent series impedance $Z_S = R_S + jX_S$ or admittance $Y_P = G_P + jB_P$. Hence, at each node we can find Q_n as the ratio of the absolute value of the reactance X_S to the corresponding resistance R_S

$$Q_n = \frac{|X_S|}{R_S} \tag{8.10}$$

or as the ratio of the absolute value of susceptance B_P to the conductance G_P

$$Q_n = \frac{|B_P|}{G_P} \tag{8.11}$$

Using (8.10) and (8.11) and the impedance transformations in Figure 8-8(a), we can deduce that for the matching network shown in Figure 8-8(c) the maximum nodal quality factor is obtained at point B where the normalized impedance is $1 - j1.23$, resulting in

$$Q_n = |1.23|/1 = 1.23 \tag{8.12}$$

To relate the nodal quality factor Q_n to Q_L, we compare the result of (8.12) with (8.9) and find

$$Q_L = \frac{Q_n}{2} \tag{8.13}$$

This result is true for any L-type matching network. For more complicated configurations the loaded quality factor of the matching network is usually estimated as simply the maximum nodal quality factor. Even though this approach does not yield a quantitative estimate of the circuit bandwidth, it nonetheless allows us to compare networks qualitatively and to select a network with higher or lower bandwidth.

To simplify the matching network design process even further we can draw constant-Q_n contours in the Smith Chart. Figure 8-11 shows such contours for Q_n valued 0.3, 1, 3, and 10.

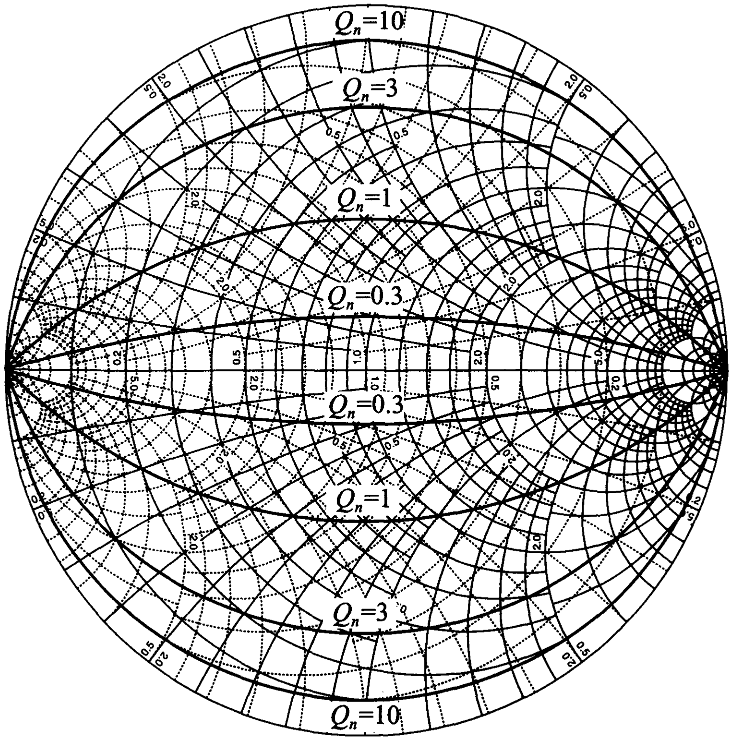

Figure 8-11 Constant Q_n contours displayed in the Smith Chart.

To obtain the equations for these contours we refer back to the general derivation of the Smith Chart in Chapter 3. There it is shown in (3.6) and (3.7) that the normalized impedance can be written as

$$z = r + jx = \frac{1 - \Gamma_r^2 - \Gamma_i^2}{(1 - \Gamma_r)^2 + \Gamma_i^2} + j\frac{2\Gamma_i}{(1 - \Gamma_r)^2 + \Gamma_i^2} \tag{8.14}$$

Thus, the nodal quality factor can be written as

$$Q_n = \frac{|x|}{r} = \frac{2|\Gamma_i|}{1 - \Gamma_r^2 - \Gamma_i^2} \tag{8.15}$$

Rearranging terms in (8.15), it follows that a circle equation is found in the form

$$\Gamma_i^2 + \left(\Gamma_r \pm \frac{1}{Q_n}\right)^2 = 1 + \frac{1}{Q_n^2} \tag{8.16}$$

where the "plus" sign is taken for positive reactance x and the "minus" sign for negative x.

With these constant Q_n circles in the Smith Chart it is possible to find the loaded quality factor of an L-type matching network by simply reading the corresponding Q_n and dividing it by 2. This procedure is discussed in Example 8-4.

RF&MW→

Example 8-4: Design of narrow-band matching network

Using the forbidden regions in Figure 8-7, design two L-type networks that match a $Z_L = (25 + j20)\Omega$ load impedance to a 50 Ω source at 1 GHz. Determine the loaded quality factors of these networks from the Smith Chart and compare them to the bandwidth obtained from their frequency response. Assume that the load consists of a resistance and inductance connected in series.

Solution: As we see from Figure 8-7, the normalized load impedance $z_L = 0.5 + j0.4$ lies inside of the constant conductance circle $g = 1$. There are two L-type matching networks that satisfy our requirements. The first consists of a series inductor and shunt capacitor, as shown in Figure 8-7(a), and the second is a series capacitor with shunt inductor, as shown in Figure 8-7(b). Following the same procedure as described in Example 8-2, we obtain the two matching networks shown in Figure 8-12.

According to Figure 8-12(a), the nodal quality factor for both networks is equal to $Q_n = 1$. Thus, we can expect that the bandwidth should be equal to $BW = f_0/Q_L = 2f_0/Q_n = 2$ GHz. This is checked by plotting the corresponding frequency responses for the designed matching networks, as depicted in Figure 8-13.

We observe that the bandwidth for the network corresponding to Figure 8-12(c) is approximately $BW_c = 2.4$ GHz. Interestingly, the matching network corresponding to Figure 8-12(b) does not possess a lower cut-off frequency. However, if we assume that the frequency

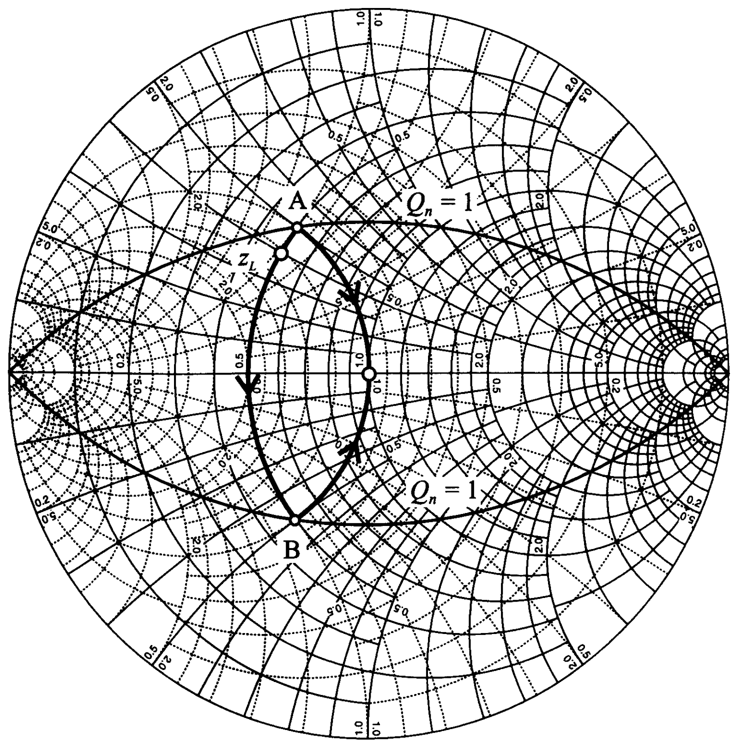

(a) Impedance transformation in the Smith Chart

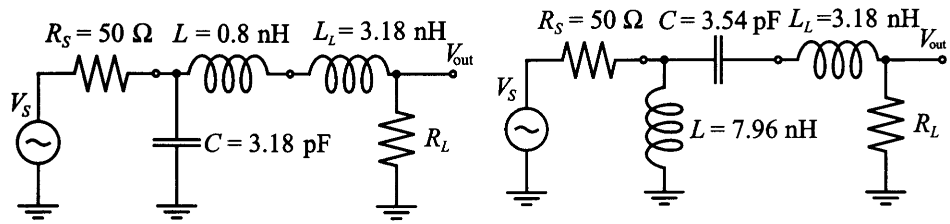

(b) (c)

Resulting matching networks

Figure 8-12 Two L-type matching networks for a 50 Ω source and a $Z_L = (25 + j20)\Omega$ load impedance operated at a frequency of 1 GHz.

response is symmetric around the resonance frequency $f_0 = 1$ GHz, then the bandwidth will be $BW_b = 2(f_{max} - f_0) = 1.9$ GHz, with the upper cut-off frequency being $f_{max} = 1.95$ GHz.

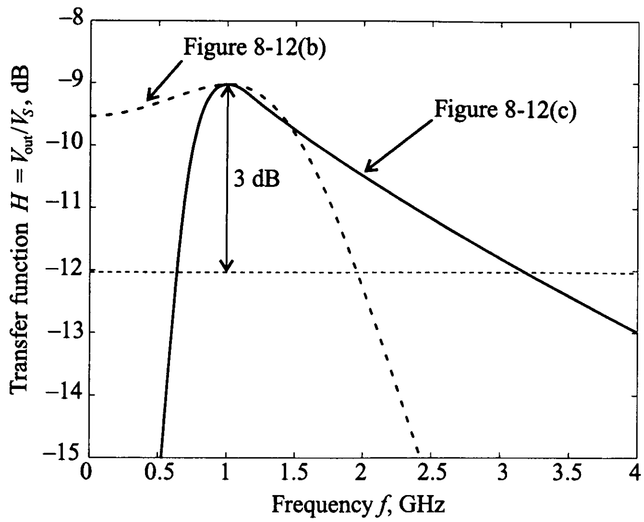

Figure 8-13 Frequency responses for the two matching networks.

Despite their design for the same resonance frequency, certain matching network configurations exhibit better high or low frequency rejection, as Figure 8-13 exemplifies.

In many practical applications the quality factor of the matching network is of importance. For example, if we design a broadband amplifier we would like to utilize networks with low Q in order to increase the bandwidth. However, for oscillator design it is desirable to achieve high-Q networks to eliminate unwanted harmonics in the output signal. Unfortunately, as we have seen in the previous example, L-type matching networks provide no control over the value of Q_n and we must either accept or reject the resulting quality factor. To gain the freedom of choosing the values of Q and thus affect the bandwidth behavior of the circuit, we can introduce a third element in the matching network. The addition of this third element results in either a T- or Pi-network, both of which are discussed next.

8.1.3 T and Pi Matching Networks

As already pointed out, the loaded quality factor of the matching network can be estimated from the maximum nodal Q_n. The addition of the third element into the matching network produces an additional node in the circuit and allows us to control the value of Q_L by choosing an appropriate impedance at that node.

The following two examples illustrate the design of T- and Pi-type matching networks with specified Q_n factor.

RF&MW

Example 8-5: Design of a T matching network

Design a T-type matching network that transforms a load impedance $Z_L = (60 - j30)\Omega$ into a $Z_{\text{in}} = (10 + j20)\Omega$ input impedance and that has a maximum nodal quality factor of 3. Compute the values for the matching network components, assuming that matching is required at $f = 1$ GHz.

Solution: There are several possible solutions that satisfy the design specifications. In this example, we investigate only one design since the rest can easily be obtained by using the same approach.

The general topology of the T-type matching network is shown in Figure 8-14.

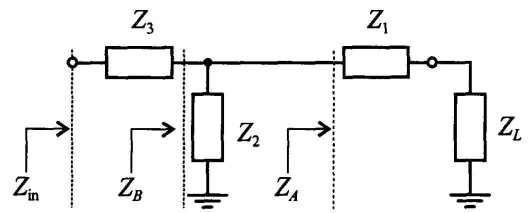

Figure 8-14 General topology of a T-type matching network.

The first element in this network is connected in series with the load impedance. Because Z_1 is purely reactive, the combined impedance Z_A will reside somewhere on the constant resistance circle described by $r = r_L$. Similarly, Z_3 is connected in series with the input so that the combined impedance Z_B (consisting of Z_L, Z_1, and Z_2) is positioned somewhere on the constant resistance circle with $r = r_{\text{in}}$. Because the network should have a nodal quality factor $Q_n = 3$, we can choose the impedance values in such a way that Z_B is located on the intersection of the constant resistance circle $r = r_{\text{in}}$ and the $Q_n = 3$ circle (see point B in Figure 8-15).

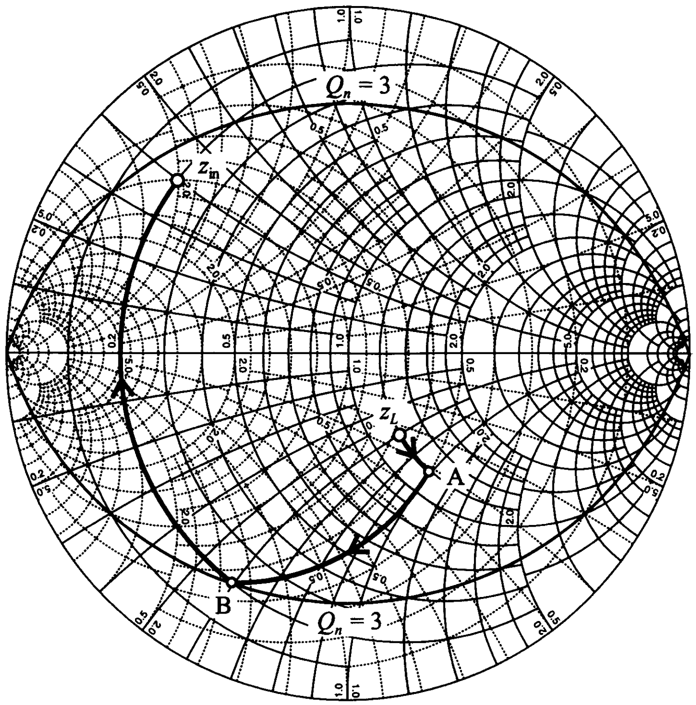

Figure 8-15 Design of a T-type matching network for a specified $Q_n = 3$.

We next find the intersection point A of the constant conductance circle that passes through the point B obtained from the previous step. The circle of constant resistance $r = r_L$ now allows us to determine the required value of the remaining component of the network to reach the point z_{in}.

The complete T-type matching network with the actual component values is illustrated in Figure 8-16. The computed elements are based on the required matching frequency of $f = 1$ GHz.

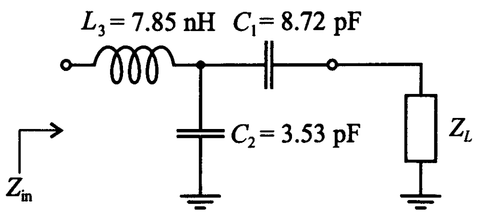

Figure 8-16 T-type matching network circuit schematics.

The extra degree of freedom to adjust the quality factor (bandwidth) of a matching network comes at the expense of an additional circuit element.

In the following example the design of a Pi-type matching network is developed with the intent to achieve a minimum nodal quality factor. A low quality factor design directly translates into a wider bandwidth of the network, as required, for instance, in broadband FET and BJT amplifiers.

Example 8-6: Design of a Pi-type matching network

For a broadband amplifier it is required to develop a Pi-type matching network that transforms a load impedance of $Z_L = (10 - j10)\Omega$ into an input impedance of $Z_{in} = (20 + j40)\Omega$. The design should involve the lowest possible nodal quality factor. Find the component values, assuming that matching should be achieved at a frequency of $f = 2.4$ GHz.

Solution: Since the load and input impedances are fixed, we cannot produce a matching network that has a quality factor lower than the highest Q_n computed at the locations Z_L and Z_{in}. Therefore, the minimum value for Q_n is determined at the input impedance location as $Q_n = |X_{in}|/R_{in} = 40/20 = 2$. The Smith Chart design of the Pi-type matching network based on $Q_n = 2$ is depicted in Figure 8-17.

In the design we employ a method very similar to the one used in Example 8-5. First, we plot a constant conductance circle $g = g_{in}$ and find its intersection with the $Q_n = 2$ contour in the Smith Chart. This intersection is denoted as point B. Next, we find the intersection point of the constant conductance circle $g = g_L$ with the constant resistance circle that passes through the point B. The resulting point is denoted as A in Figure 8-17.

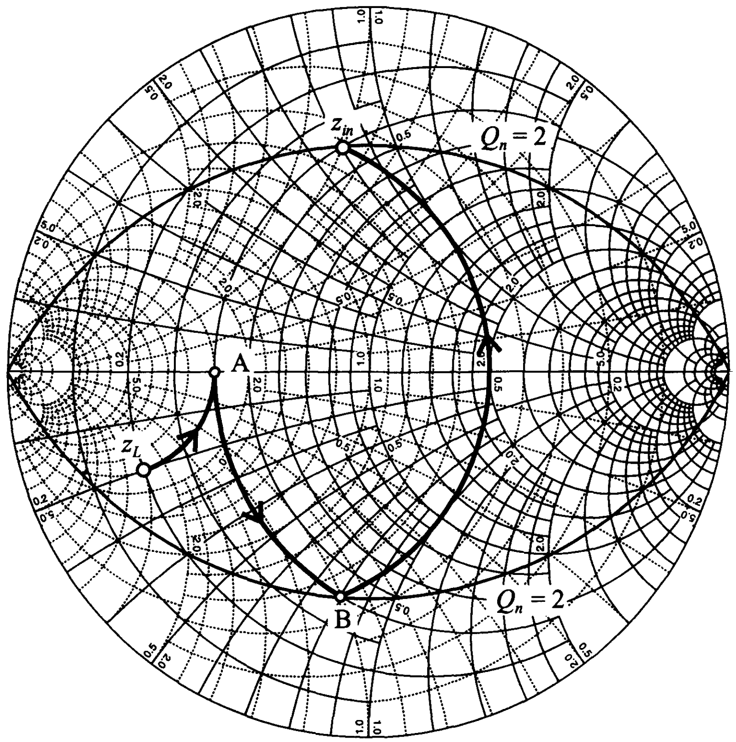

Figure 8-17 Design of a Pi-type matching network using a minimal Q_n.

The network components can be determined based on converting the Smith Chart points into actual capacitances and inductances as detailed in Example 8-2. The resulting circuit configuration is shown in Figure 8-18.

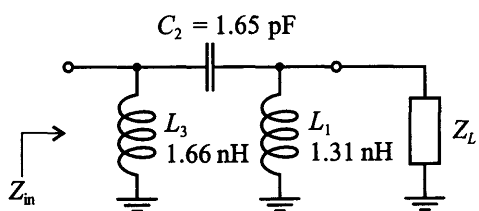

Figure 8-18 Pi-type matching network configuration.

It is interesting to note that unlike the situation discussed in Example 8-5, the relative positions of Z_L and Z_{in} in this example are such that only one possible Pi-type network configuration with

$Q_n = 2$ exists. All other realizations of the Pi-type network will result in an increased nodal quality factor. Furthermore, if we had a lower load resistance, we would not be able to implement this Pi-type network for the given Q_n.

As this example shows, the bandwidth cannot be increased arbitrarily by reducing the nodal quality factor. The limits are set by the desired input and output impedances.

8.2 Microstrip Line Matching Networks

In the previous sections we have discussed the design of matching networks involving discrete components. However, with increasing frequency and correspondingly reduced wavelength, the influence of parasitics in the discrete elements becomes more noticeable. The design now requires us to take these parasitics into account, thus significantly complicating the component value computations. This, along with the fact that discrete components are only available for certain values, limits their use in high-frequency circuit applications. As an alternative to lumped elements, distributed components are widely used when the wavelength becomes sufficiently small compared with the characteristic circuit component length, a fact already discussed in Chapter 2.

8.2.1 From Discrete Components to Microstrip Lines

In the mid-GHz range, design engineers often employ a mixed approach by combining lumped and distributed elements. These types of matching networks usually contain a number of transmission lines connected in series and capacitors spaced in a parallel configuration, as illustrated in Figure 8-19. The reader is also referred to Figure 1-2(a) for a practical example.

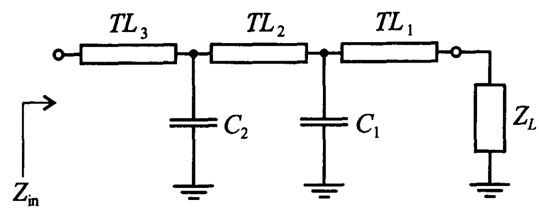

Figure 8-19 Mixed design of matching network involving transmission line sections (TL) and discrete capacitive elements.

Inductors are usually avoided in such designs because they tend to have higher resistive losses than capacitors. In general, only one shunt capacitor with two transmission lines connected in series on both sides is sufficient to transform any given load impedance to any input impedance. Similar to the L-type matching networks, such configurations may involve the additional requirement of a fixed Q_n, necessitating additional components to control the quality factor of the circuit.

The arrangement of components shown in Figure 8-19 is very attractive in practice, since it permits tuning the circuit after it has been manufactured. Changing the values of the capacitors as well as placing them at different locations along the transmission lines offers a wide range of flexibility. The tuning capability makes these types of matching networks very popular for prototyping. Usually, all transmission lines have the same width (i.e., the same characteristic impedance) to simplify the actual tuning.

Example 8-7 discusses the Smith Chart approach to the design of a matching network containing two 50 Ω transmission lines connected in series and a single shunt capacitor placed in-between them.

RF&MW

Example 8-7: Design of a matching network with lumped and distributed components

Design a matching network that transforms the load $Z_L = (30 + j10)\Omega$ to an input impedance $Z_{\text{in}} = (60 + j80)\Omega$. The matching network should contain only two series transmission lines and a shunt capacitance. Both transmission lines have a 50 Ω characteristic line impedance, and the frequency at which matching is desired is $f = 1.5$ GHz.

Solution: The first step involves identifying the normalized load impedance $z_L = 0.6 + j0.2$ as a point in the Smith Chart. We can then draw a SWR circle that indicates the combined impedance of the load connected to the 50 Ω transmission line. The position on the SWR circle is determined by the length of the transmission line, as investigated in Chapter 3.

The second step requires plotting a SWR circle that passes through the normalized input impedance point $z_{\text{in}} = 1.2 + j1.6$ shown in Figure 8-20.

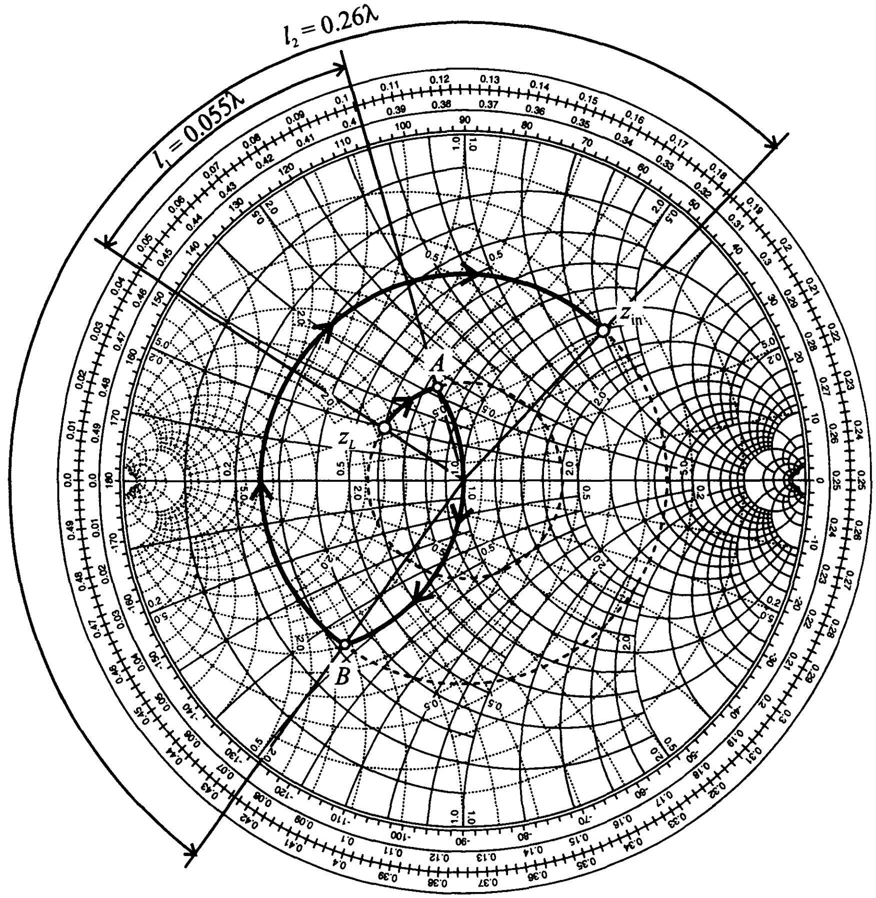

Figure 8-20 Design of the distributed matching network for Example 8-7.

The choice of the point from which we transition from the load SWR circle to the input SWR circle can be made arbitrarily. In Figure 8-20 the point A is chosen, which approximately corresponds to a normalized admittance value of $y_A = 1 - j0.6$. The addition of the parallel capacitor results in the movement along the circle of constant conductance $g = 1$ and transforms the impedance from point A to point B on the input SWR circle of the Smith Chart. From point B an impedance transformation is required along the constant SWR circle by adding a series connected transmission line.

As a final step, the electrical length of the transmission lines must be determined. This can be done by reading the two lengths l_1,

l_2 from the so-called **WTG** (wavelength toward generator) scale displayed on the outer perimeter of the Smith Chart (see Figure 8-20). The resulting circuit schematics for the matching network is shown in Figure 8-21

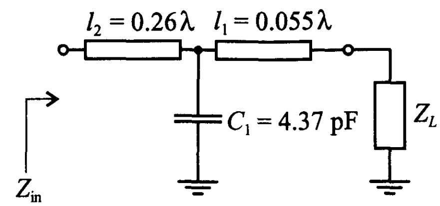

Figure 8-21 Matching network combining series transmission lines and shunt capacitance.

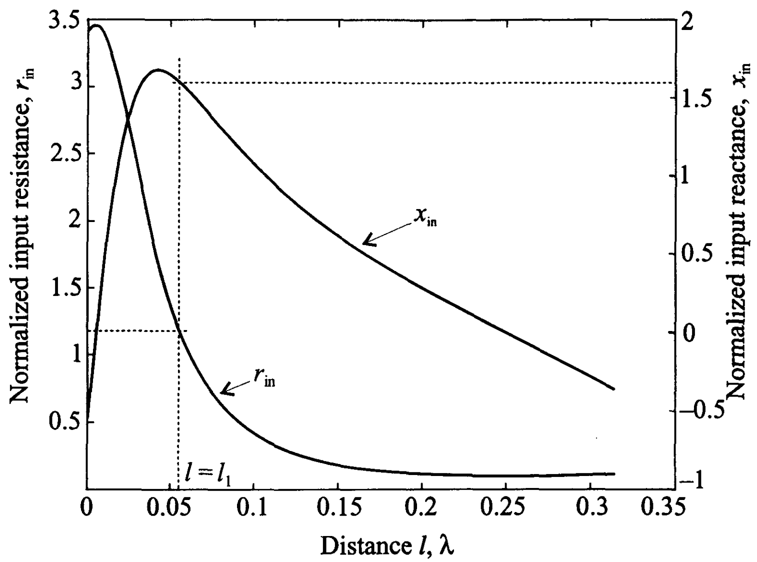

Figure 8-22 Input impedance as a function of the position of the shunt capacitor in Example 8-7.

It is interesting to investigate the tuning capability range for this circuit configuration. Figure 8-22 shows the dependency of the real r_{in} and imaginary x_{in} parts of the input impedance as a function of the distance l between the load and the capacitor location. In other words, the total length $l_1 + l_2$ is kept fixed and the placement of the capacitor is varied from the load end to the beginning of the network (i.e., $0 \le l \le l_1 + l_2$). The dashed lines indicate the original design. It is noticed that x_{in} undergoes the expected inductive (positive values) to capacitive (negative values) transition.

In this example we have designed a combined matching network that involves both distributed (transmission lines) and a lumped (capacitor) element. These types of networks have rather large tuning capabilities, but are very sensitive to the placement of the capacitor along the transmission line. Even small deviations from the target location result in drastic changes in the input impedance.

8.2.2 Single-Stub Matching Networks

The next logical step in the transition from lumped to distributed element networks is the complete elimination of all lumped components. This is accomplished by employing open- and/or short-circuit stub lines.

In this section we consider matching networks that consist of a series transmission line connected to a parallel open-circuit or short-circuit stub. Let us investigate two topologies: The first one involves a series transmission line connected to the parallel combination of load and stub, as shown in Figure 8-23(a), and the second involves a parallel stub connected to the series combination of the load and transmission line, as depicted in Figure 8-23(b).

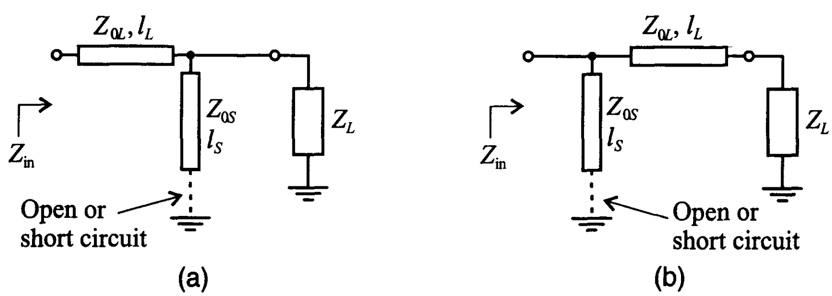

Figure 8-23 Two topologies of single-stub matching networks.

The matching networks in Figure 8-23 possess four adjustable parameters: length l_S and characteristic impedance Z_{0S} of the stub, and length l_L and characteristic impedance Z_{0L} of the transmission line.

Example 8-8 demonstrates the design procedure for the matching network topology shown in Figure 8-23(a) with the characteristic impedances of both stub Z_{0S} and transmission line Z_{0L} fixed to the same arbitrary value Z_0 and their electrical lengths variable to meet the particular input impedance requirement.

RF&MW→

Example 8-8: Single-stub matching network design with fixed characteristic impedances

For a load impedance of $Z_L = (60 - j45)\Omega$, design two single-stub matching networks that transform the load to a $Z_{\text{in}} = (75 + j90)\Omega$ input impedance. Assume that both stub and transmission line in Figure 8-23(a) have a characteristic impedance of $Z_0 = 75\ \Omega$.

Solution: The basic concept is to select the length l_S of the stub such that it produces a susceptance B_S sufficient to move the load admittance $y_L = 0.8 + j0.6$ to the SWR circle that passes through the normalized input impedance point $z_{\text{in}} = 1 + j1.2$, as illustrated in Figure 8-24.

We notice that the input SWR circle associated with $z_{\text{in}} = 1 + j1.2$ intersects the constant conductance circle $g = 0.8$ in two points (at $y_A = 0.8 + j1.05$ and at $y_B = 0.8 - j1.05$) suggesting two possible solutions. The corresponding susceptance values for the stub are $jb_{SA} = y_A - y_L = j0.45$ and $jb_{SB} = y_B - y_L = -j1.65$, respectively. In the first case, the length of an open-circuit stub can be found in the Smith Chart by measuring the length l_{SA}, starting from the $y = 0$ point (open circuit) and moving along the outer perimeter of the Smith Chart $g = 0$ toward the generator (clockwise) to the point where $y = j0.45$. The length for this case is $l_{SA} = 0.067\lambda$. The open-circuit stub can be replaced by a short-circuit stub if its length is increased by a quarter wavelength. Such a substitution may become necessary if a coaxial cable is used because of excessive radiation losses due to the large cross-sectional area. In printed circuit design, open-circuit stubs are sometimes preferred because they eliminate the deployment of a via,

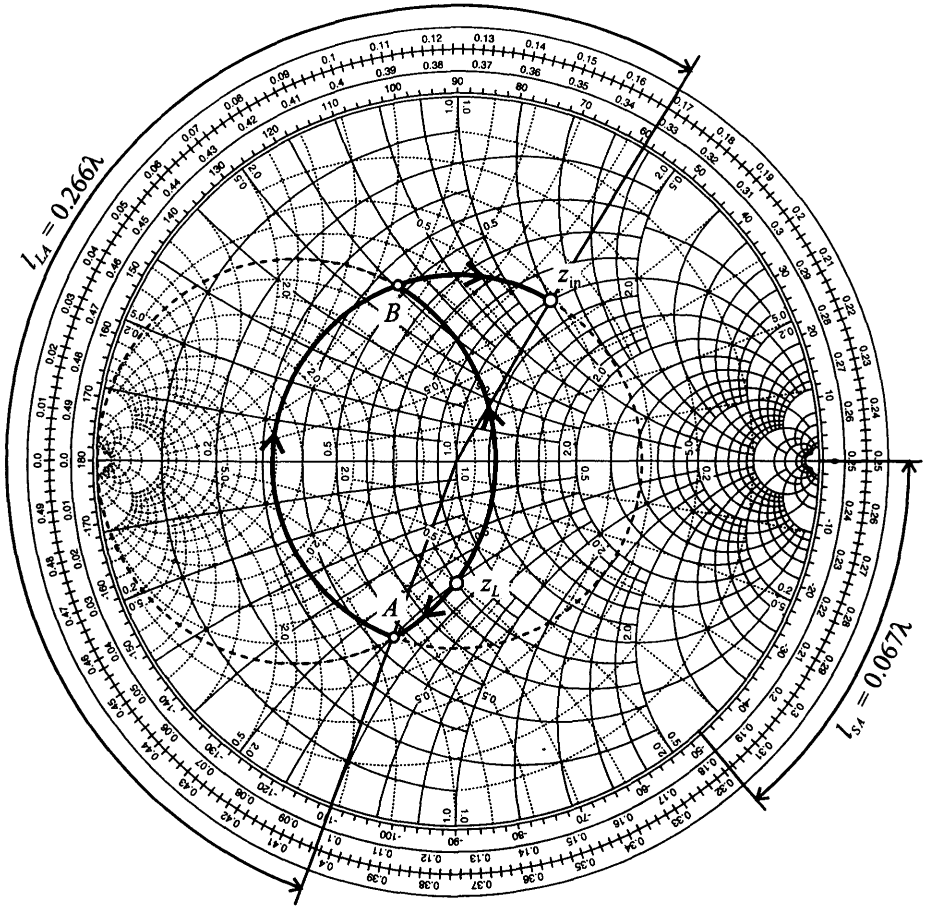

Figure 8-24 Smith Chart design for the single-stub matching network based on Example 8-8.

which is otherwise necessary to obtain the ground connection for a short-circuit stub.

Similar to the first solution, b_{SB} yields the length $l_{SB} = 0.337\lambda$ for the open-circuit stub, and $l_{SB} = 0.087\lambda$ for the short-circuit stub. For this case we also notice that creating a short-circuit stub requires a shorter length than an open-circuit stub. This is due to the fact that the open-circuit stub models a negative susceptance.

The length of the series transmission line segment is found in the same way as described in Example 8-7 and is equal to

$l_{LA} = 0.266\lambda$ for the first solution and $l_{LB} = 0.07\lambda$ for the second solution.

A circuit designer often has to minimize the size of the circuit board and therefore must be concerned about employing the shortest possible transmission line segments. Depending on the impedance requirements, this can either be an open- or short-circuit stub section.

In the next example we illustrate the generic design procedure for the matching network topology shown in Figure 8-23(b). Unlike the previous example, we now fix the lengths of both the stub and the transmission line segment but vary their characteristic impedances. In a microstrip line circuit design this is typically accomplished by changing the width of the lines.

RF&MW→

Example 8-9: Design of a single-stub matching network using transmission lines with different characteristic impedances

Using the matching network topology shown in Figure 8-23(b), choose the characteristic impedances of the stub and transmission line such that the load impedance $Z_L = (120 - j20)\Omega$ is transformed into the input impedance $Z_{in} = (40 + j30)\Omega$. Assume that the length of the transmission line is $l_L = 0.25\lambda$ and the stub has the length of $l_S = 0.375\lambda$. Furthermore, determine whether a short-circuit or an open-circuit stub is necessary for this circuit.

Solution: The combined impedance Z_1 of the series connection of the load impedance with the transmission line can be computed using the formula for the quarter-wave transformer:

$$Z_1 = Z_{0L}^2/Z_L \tag{8.17}$$

The addition of the open-circuit stub results in an input admittance of

$$Y_{\text{in}} = Y_1 + jB_S \tag{8.18}$$

where $Y_1 = Z_1^{-1}$ is the admittance of the previously computed series combination of load impedance and transmission line and $jB_S = \pm jZ_{0S}^{-1}$ is the susceptance of the stub. The "plus" or "minus" signs correspond to either a short-circuit or an open-circuit stub.

Combining (8.17) and (8.18), we find

$$G_{\text{in}} = R_L/Z_{0L}^2 \tag{8.19a}$$

$$B_{\text{in}} = X_L/Z_{0L}^2 \pm Z_{0S}^{-1} \tag{8.19b}$$

where we have used the input admittance and load impedance representation in terms of their real and imaginary components: $Y_{\text{in}} = G_{\text{in}} + jB_{\text{in}}$, $Z_L = R_L + jX_L$.

Using (8.19a), we find the characteristic impedance of the transmission line to be

$$Z_{0L} = \sqrt{\frac{R_L}{G_{\text{in}}}} = \sqrt{\frac{120}{0.016}} = 86.6\ \Omega$$

Substituting the obtained value into (8.19b), we find that the "minus" sign should be used; that is, we need to implement an open-circuit stub with a characteristic impedance of

$$Z_{0S} = \frac{1}{X_L/Z_{0L}^2 - B_{\text{in}}} = 107.1\ \Omega$$

This design approach is very easy to implement as long as the characteristic impedance stays within reasonable limits ranging approximately from 20 to 200 Ω.

In practical realizations single-sided unbalanced stubs are often replaced by the balanced design, as shown in Figure 8-25.

Naturally, the combined susceptance of the parallel connection of stubs $ST1$ and $ST2$ has to be equal to the susceptance of the unbalanced stub. Therefore, the susceptance of each side of the balanced stub must be equal to half of the susceptance of the

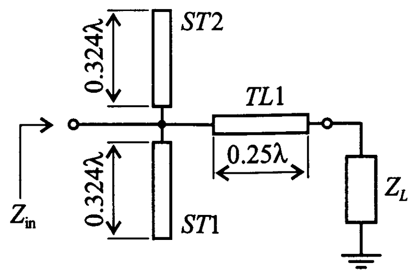

Figure 8-25 Balanced stub design for Example 8-9.

unbalanced stub. We note that the length l_{SB} of each side does not scale linearly. In other words, the length of the balanced stub is not half of the length of the unbalanced stub l_S. Rather, it has to be computed as

$$l_{SB} = \frac{\lambda}{2\pi}\tan^{-1}\left(2\tan\frac{2\pi l_S}{\lambda}\right) \tag{8.20}$$

for open-circuit stub, or

$$l_{SB} = \frac{\lambda}{2\pi}\tan^{-1}\left(\frac{1}{2}\tan\frac{2\pi l_S}{\lambda}\right) \tag{8.21}$$

for short-circuit stub. This result can also be found graphically by using the Smith Chart.

8.2.3 Double-Stub Matching Networks

The single-stub matching networks in the previous section are quite versatile and allow matching between any input and load impedances, so long as they have a nonzero real part. One of the main drawbacks of such matching networks is that they require a variable-length transmission line between stub and input port, or between stub and load impedance. Usually this does not pose a problem for fixed networks, but it may create difficulties for variable tuners. In this section we examine matching networks that overcome this drawback by incorporating a second stub. The general topology of such a network that matches an arbitrary load impedance to an input impedance $Z_{in} = Z_0$ is shown in Figure 8-26.

In double-stub matching networks two short- or open-circuit stubs are connected in parallel with a fixed-length transmission line placed in between. The length l_2 of this line is usually chosen to be one-eighth, three-eighth, or five-eighth of a wavelength. The

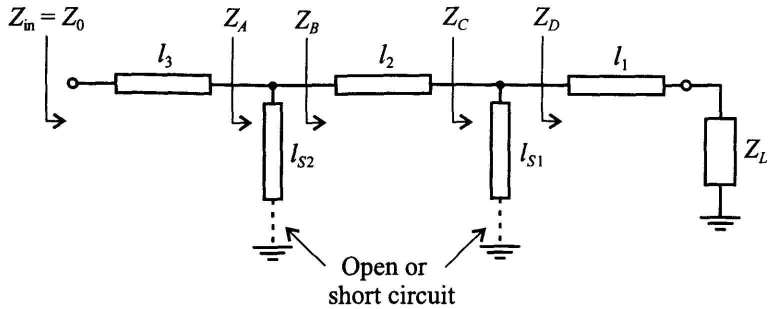

Figure 8-26 Double-stub matching network arrangement.

three-eighth and five-eighth wavelength spacings are typically employed in high-frequency applications to simplify the tuner construction.

Let us assume for our subsequent discussion that the length of the line segment between the two stubs is $l_2 = (3/8)\lambda$. To facilitate the analysis we start from the input side of the tuner and work backward to the load end.

For a perfect match it is required that $Z_{in} = Z_0$ and therefore $y_A = 1$. Since it is assumed that the lines are lossless, the normalized admittance $y_B = y_A - jb_{S2}$ is located somewhere on the constant conductance circle $g = 1$ in the Smith Chart. Here b_{S2} is the susceptance of the stub and l_{S2} is the associated length. For an $l_2 = (3/8)\lambda$ line the $g = 1$ circle is rotated by $2\beta l_2 = 3\pi/2$ radians or 270° toward the load (i.e., in counter-clockwise direction, as depicted in Figure 8-27). The admittance y_C (being the series connection of Z_L with line l_1 in parallel to stub l_{S1}) needs to reside on this rotated $g = 1$ circle (called the y_C circle) in order to ensure matching.

By varying the length of the l_{S1} stub we can transform point y_D in such a way that the resulting y_C is indeed located on the rotated $g = 1$ circle. This procedure can be done for any load impedance except for the case when point y_D (i.e., the series connection of Z_L and line l_1) is located inside the $g = 2$ circle. This represents the forbidden region that has to be avoided. To overcome this problem in practical applications, commercial double-stub tuners usually have input and output transmission lines whose lengths are related according to $l_1 = l_3 \pm \lambda/4$. In this case, if a particular load impedance cannot be matched, one simply connects the load to the opposite end of the tuner, which moves y_D out of the forbidden region.

The following example demonstrates the computation of the stub lengths to achieve matching for a specific load impedance.

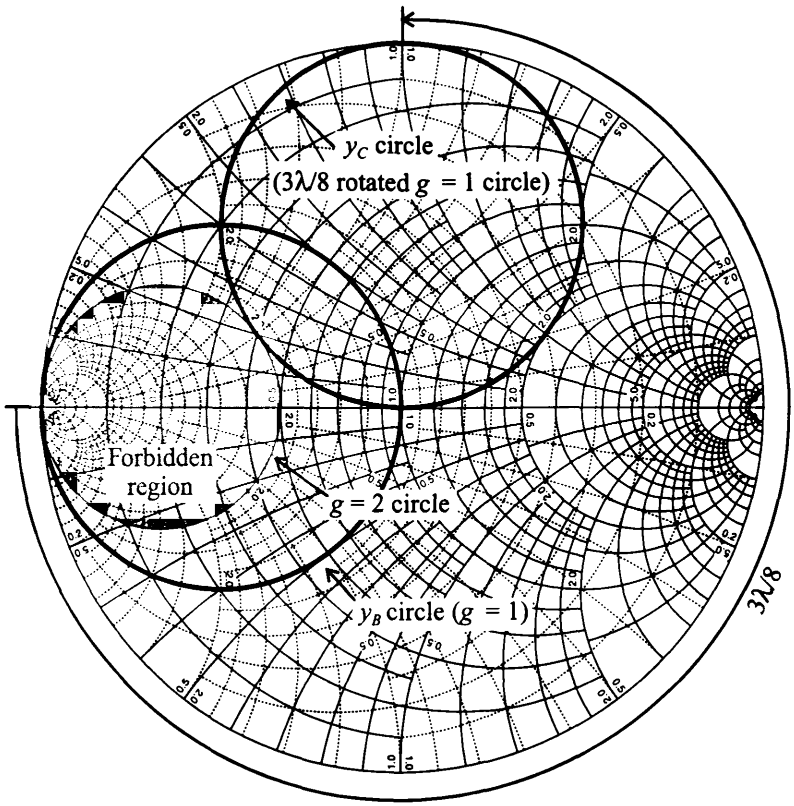

Figure 8-27 Smith Chart analysis of a double-stub matching network shown in Figure 8-26.

RF&MW

Example 8-10: Design of a double-stub matching network

It is assumed that in the double-stub matching network shown in Figure 8-26 the lengths of the transmission lines are $l_3 = l_2 = 3\lambda/8$ and $l_1 = \lambda/8$. Find the lengths of the short-circuit stubs that match the load impedance $Z_L = (50 + j50)\Omega$ to a 50 Ω input impedance. The characteristic line impedance for all components is $Z_0 = 50\ \Omega$.

Solution: First the normalized admittance y_D has to be determined and checked that it does not fall inside the forbidden region. Using the Smith Chart (see Figure 8-28), we find $y_D = 0.4 + j0.2$. Since $g_D < 2$, we are assured that the admittance y_D does not fall into the forbidden region. Next we plot the rotated $g = 1$ circle as explained previously. This allows us to fix the intersection of the rotated $g = 1$ circle with the constant conductance circle that passes through the point y_D. The intersection point gives us the value of y_C. In fact, there are two intersection points that yield two possible solutions. If we choose $y_C = 0.4 - j1.8$, then the susceptance of the first stub should be $jb_{S1} = y_C - y_D = -j2$, which permits us to determine the length of the first short-circuit stub: $l_{S1} = 0.074\lambda$.

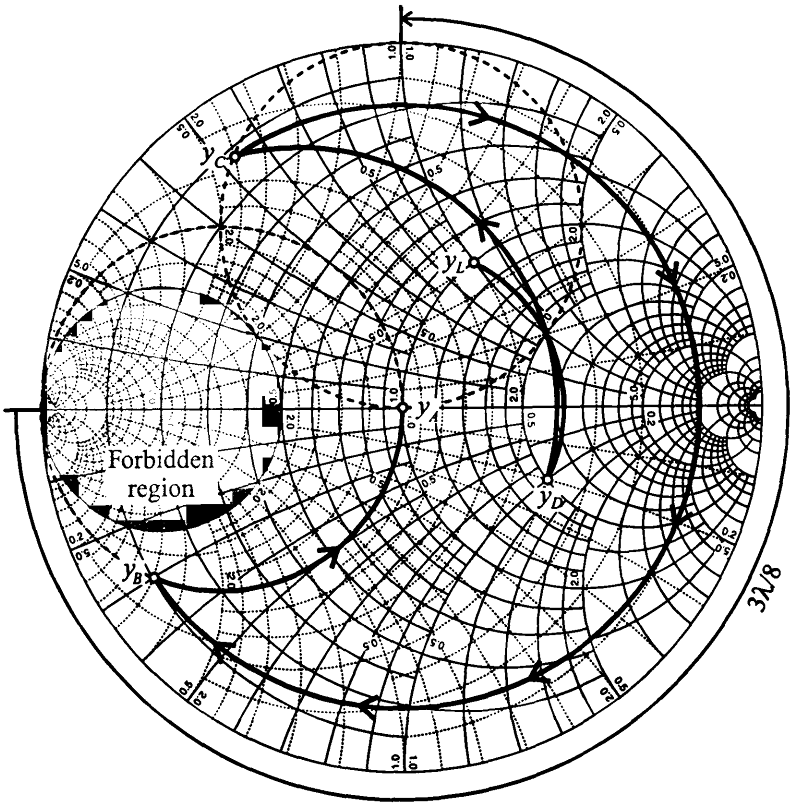

Figure 8-28 Double-stub tuning network design for Example 8-10.

Rotating y_C by $l_2 = 3\lambda/8$ we find $y_B = 1 + j3$, which means that we have to make the susceptance of the second stub equal to $jb_{S2} = -j3$ so that $y_{in} = y_A = 1$. Using the Smith Chart, we find that the length of the second stub is $l_{S2} = 0.051\lambda$.

In some practical realizations the stubs are replaced by varactor diodes. This allows an electronic tuning of the diode capacitances and thus the shunt admittances.

8.3 Amplifier Classes of Operation and Biasing Networks

An indispensable building block in any RF circuit is the active or passive biasing network. The purpose of biasing is to provide the appropriate quiescent point for the active devices under specified operating conditions and maintain a constant setting irrespective of transistor parameter variations and temperature fluctuations.

In the following section we introduce a general analysis of the different classes of amplifier operation. This will enable us to develop an understanding of how BJT and FET need to be appropriately biased.

8.3.1 Classes of Operation and Efficiency of Amplifiers

Depending on the application for which the amplifier is designed, specific bias conditions are required. There are several classes of amplifier operation that describe the biasing of an active device in an RF circuit.

In Figure 8-29 the transfer function characteristic of an ideal transistor is displayed. It is assumed that the transistor does not reach saturation or breakdown regions and in the linear operating region the output current is proportional to the input voltage. The voltage V^* corresponds either to the threshold voltage in case of FETs or the base-emitter built-in potential in case of BJTs.

The distinction between different classes of operation is made based upon the so-called **conduction angle**, which indicates the portion of the signal cycle when the current is flowing through the load. As depicted in Figure 8-29(a), in **Class A** operation the current is present during the entire output signal cycle. This corresponds to a $\Theta_A = 360°$ conduction angle. If the transfer characteristic of the transistor in the linear region is close to that of a linear function, then the output signal is an amplified replica of the input signal without suffering any distortion. In practical circuits, however,

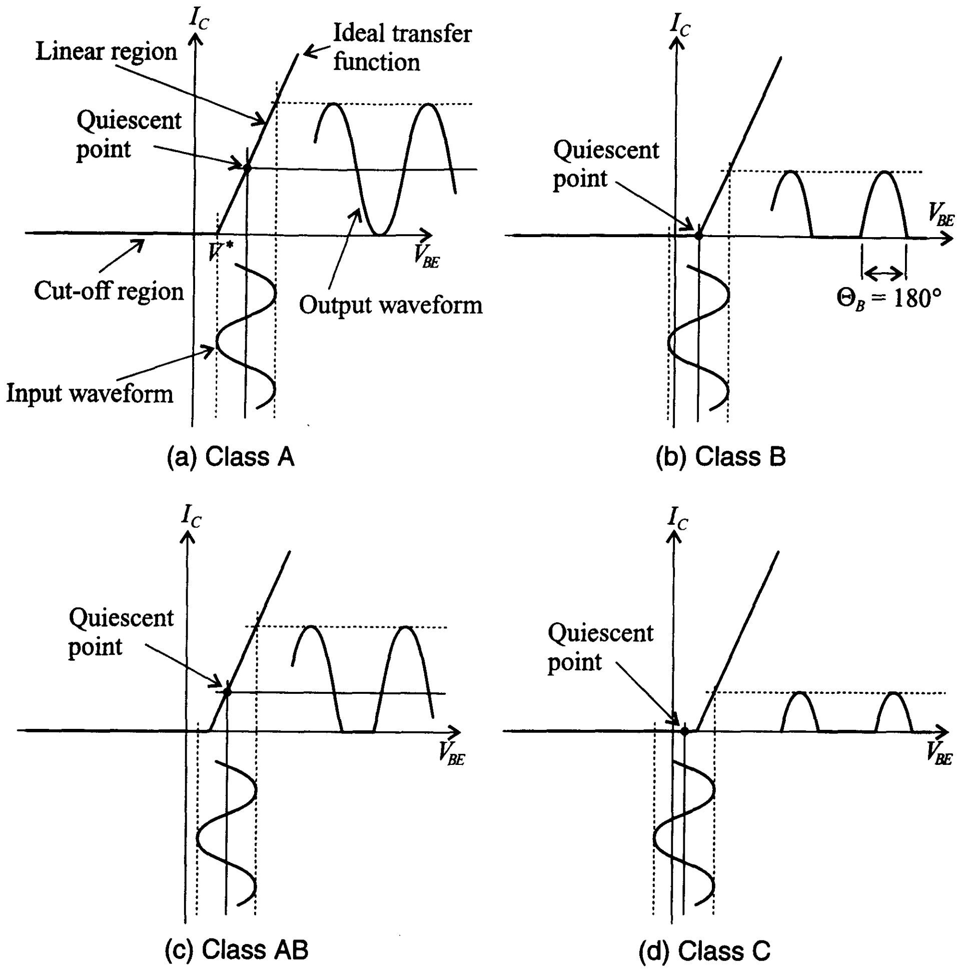

Figure 8-29 Various classes of amplifier operation.

there is always a certain degree of nonlinearity present which results in a distorted output signal of the amplifier.

In **Class B** [Figure 8-29(b)] the current is present during only half of the cycle, corresponding to a $\Theta_B = 180°$ conduction angle. During the second half of the cycle, the transistor is in the cut-off region and no current flows through the device. **Class AB** [Figure 8-29(c)] combines the properties of the classes A and B and has a conduction angle Θ_{AB} ranging from 180° to 360°. This type of amplifier is typically employed when a high-power "linear" amplification of the RF signal is required.

In a **Class C** amplifier [Figure 8-29(d)] we have a nonzero current for less than half of the cycle (i.e., the conduction angle is $0 < \Theta_C < 180°$). This results in maximum distortion of the output signal.

A logical question that arises is why are not all amplifiers operated in Class A since this mode delivers the least signal distortion? The answer is directly linked to the amplifier efficiency. Efficiency, η, is defined as the ratio of the average RF power P_{RF} delivered to the load over the average power P_S supplied by the source, and is usually measured in percent:

$$\eta = \frac{P_{\text{RF}}}{P_S} 100\% \tag{8.22}$$

The theoretical maximum efficiency of the Class A amplifier is only 50%, but the efficiency of Class C can reach values close to 100%. Fifty percent efficiency of Class A amplifiers means that half of the power supplied by the source is dissipated as heat. This situation may not be acceptable in portable communication systems where most devices are battery operated. In practical applications, designers usually choose the class of operation that gives maximum efficiency but still preserves the informational content of the RF signal.

In the following example we derive the maximum theoretical efficiency η of the amplifier as a function of conduction angle.

Example 8-11: Amplifier efficiency computation

Derive the general expression for the amplifier efficiency η as a function of conduction angle Θ_0. List the values of η for both Class A and Class B amplifiers.

Solution: The electrical current through the load for a conduction angle of Θ_0 has a waveform shown in Figure 8-30(a), where the cosine current amplitude is given by I_0.

Similarly, the power supply current I_S has a maximum value of I_0 plus the quiescent current I_Q:

$$I_S = I_Q + I_0 \cos\Theta \tag{8.23}$$

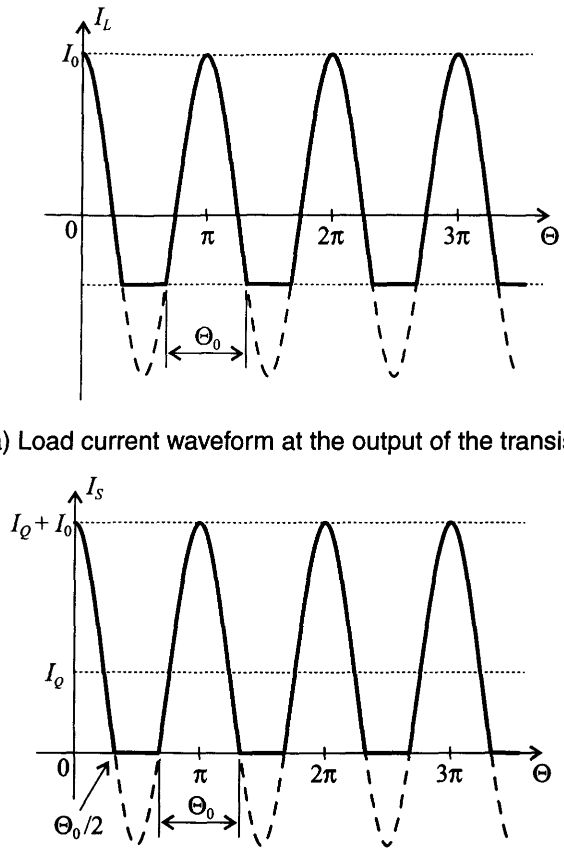

Figure 8-30 Load and power supply current waveforms as a function of conduction angle.

The value of the quiescent current necessary to ensure the specified conduction angle Θ_0 can be found from (8.23) by setting I_S to zero at $\Theta = \Theta_0/2$:

$$I_Q = -I_0\cos(\Theta_0/2) \tag{8.24}$$

The average power supply current is then computed as an integral over the conduction angle ranging between the limits of $\Theta = -\Theta_0/2$ and $\Theta = \Theta_0/2$; that is,

$$\langle I_S\rangle = \frac{1}{2\pi}\int_{-\Theta_0/2}^{\Theta_0/2} I_S d\Theta = -\frac{I_0}{2\pi}\left[\Theta_0\cos\left(\frac{\Theta_0}{2}\right) - 2\sin\left(\frac{\Theta_0}{2}\right)\right] \tag{8.25}$$

Thus, the average power from the power supply is

$$P_S = V_{CC}\langle I_S\rangle = -\frac{I_0 V_{CC}}{2\pi}\left[\Theta_0\cos\left(\frac{\Theta_0}{2}\right) - 2\sin\left(\frac{\Theta_0}{2}\right)\right] \quad (8.26)$$

where V_{CC} is the supply voltage.

Since the voltage on the load changes together with the current, the average RF power is computed as an integral of the product of load current and load voltage:

$$P_{RF} = \frac{1}{2\pi}\int_{-\Theta_0/2}^{\Theta_0/2} I_0 V_{CC}\cos^2\Theta d\Theta = \frac{I_0 V_{CC}}{4\pi}(\Theta_0 - \sin\Theta_0) \quad (8.27)$$

Dividing (8.27) by (8.26), we find an amplifier efficiency

$$\eta = -\frac{\Theta_0 - \sin\Theta_0}{2[\Theta_0\cos(\Theta_0/2) - 2\sin(\Theta_0/2)]} \quad (8.28)$$

where the conduction angle Θ_0 is measured in radians.

The graph of η as a function of the conduction angle Θ_0 is shown in Figure 8-31.

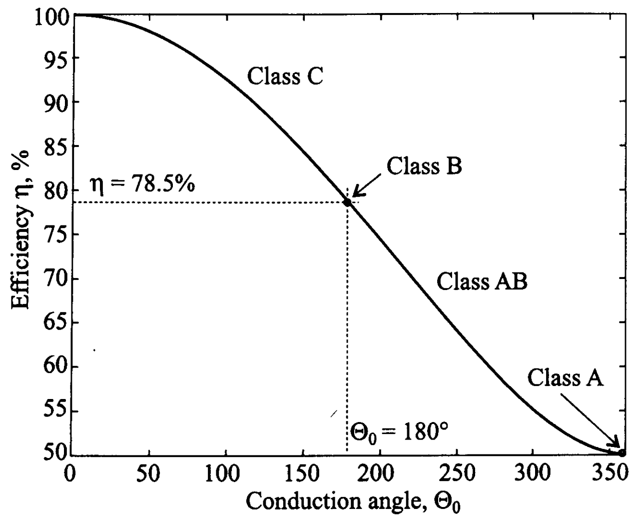

Figure 8-31 Maximum theoretical efficiency of an ideal amplifier as a function of conduction angle.

Substituting $\Theta_0 = 2\pi$ into (8.28), we find that the efficiency of a Class A amplifier is indeed 50%. To determine the efficiency of a Class B amplifier, we simply use the conduction angle $\Theta_0 = \pi$ in (8.28), which yields

$$\eta_B = -\frac{\pi - \sin\pi}{2[\pi\cos(\pi/2) - 2\sin(\pi/2)]} = \frac{\pi}{4} = 0.785$$

That is, Class B yields an efficiency of 78.5%.

Efficiency is an important design consideration when dealing with low power consumption, as required, for instance, in personal communication systems, where battery lifetime must be maximized.

8.3.2 Bipolar Transistor Biasing Networks

There are generally two types of biasing networks: passive and active. **Passive** (or **self-biased**) networks are the simplest type of biasing circuits and usually incorporate a resistive network, which provides the appropriate voltages and currents for the RF transistor. The main disadvantages of such networks are that they are very sensitive to changes in transistor parameters and that they provide poor temperature stability. To compensate for these drawbacks **active biasing** networks are often employed.

In this section we consider several network configurations for biasing RF BJTs. Two possible topologies are shown in Figure 8-32.

The combination of the blocking capacitor C_B and the RFC connected to the base and collector terminals of the transistor in Figure 8-32 serve the purpose to isolate the

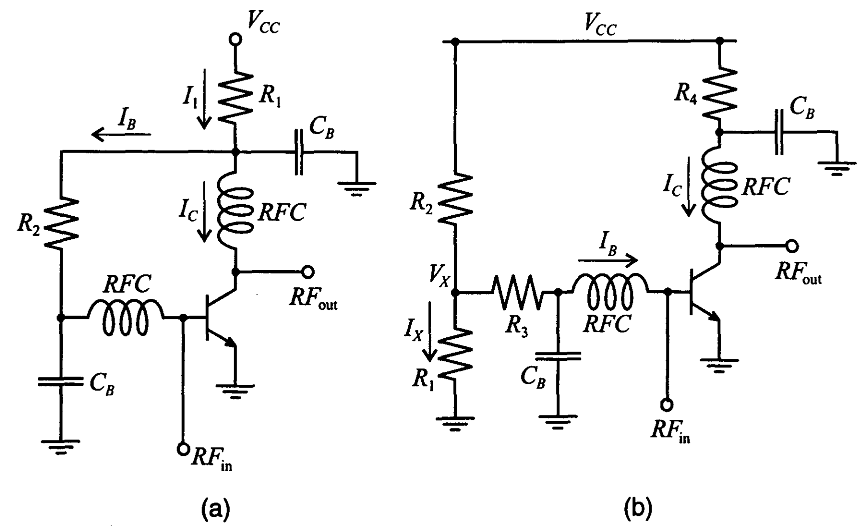

Figure 8-32 Passive biasing networks for an RF BJT in common-emitter configuration.

RF signal from the DC power source. At high frequencies, the RFCs are usually replaced by quarter wave transmission lines that convert the short-circuit condition on the C_B side to an open-circuit condition on the transistor side.

The following example discusses how to compute the resistors for the two biasing networks shown in Figure 8-32.

RF&MW→

Example 8-12: Design of passive biasing networks for a BJT in common-emitter configuration

Design biasing networks according to Figures 8-32(a) and (b) for the BJT settings of $I_C = 10$ mA, $V_{CE} = 3$ V, and $V_{CC} = 5$ V. Assume that the transistor has a $\beta = 100$ and $V_{BE} = 0.8$ V.

Solution: As seen in Figure 8-32(a), the current I_1 through resistor R_1 is equal to the sum of the collector and base currents. Since $I_B = I_C/\beta$, we obtain

$$I_1 = I_C + I_B = I_C(1+\beta^{-1}) = 10.1 \text{ mA}$$

The value of R_1 can be found as

$$R_1 = \frac{V_{CC} - V_{CE}}{I_1} = 198\ \Omega$$

Similarly, the base resistor R_2 is computed as

$$R_2 = \frac{V_{CE} - V_{BE}}{I_B} = \frac{V_{CE} - V_{BE}}{I_C/\beta} = 22\ \text{k}\Omega$$

For the circuit in Figure 8-32(b) the situation is slightly more complicated. Here we have the freedom of choosing the value of the voltage potential V_X and the current I_X through the voltage divider resistor R_2. Arbitrarily setting V_X to 1.5 V, we determine the base resistor R_3 to be

$$R_3 = \frac{V_X - V_{BE}}{I_B} = \frac{V_X - V_{BE}}{I_C/\beta} = 7\ \text{k}\Omega$$

The value of I_X is usually chosen to be 10 times larger than I_B. Therefore, $I_X = 10 I_B = 1$ mA and the values of the resistances for the voltage divider are computed as

$$R_1 = \frac{V_X}{I_X} = 1.5\ \text{k}\Omega \text{ and } R_2 = \frac{V_{CC} - V_X}{I_X + I_B} = 3.18\ \text{k}\Omega$$

Finally, the collector resistor is found as

$$R_4 = (V_{CC} - V_{CE})/I_C = 200\ \Omega$$

The freedom of selecting particular voltages and currents is in practice restricted by the need to choose electric settings that result in standardized resistance values.

An example of an active biasing network for a BJT in common-emitter configuration is shown in Figure 8-33. Here we employ a low-frequency transistor Q_1 to provide the necessary base current for the RF transistor Q_2. The resistor R_{E1} connected to the emitter of the transistor Q_1 improves stability of the quiescent point. If transistors Q_1 and Q_2 have the same thermal properties, then this biasing network also results in good temperature stability.

Example 8-13 illustrates the determination of the component values for the active biasing network depicted in Figure 8-33.

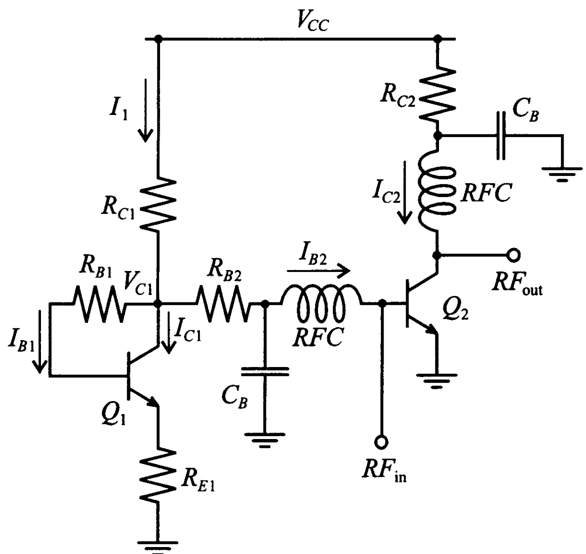

Figure 8-33 Active biasing network for a common-emitter RF BJT.

Example 8-13: Design of an active biasing network for a BJT transistor in common-emitter configuration

Design a biasing network as shown in Figure 8-33 for $I_{C2} = 10\text{ mA}$, $V_{CE2} = 3\text{ V}$, and $V_{CC} = 5\text{ V}$. Assume that both transistors have $\beta = 100$ and $V_{BE} = 0.8\text{ V}$.

Solution: Similar to the previous example we have several degrees of freedom in this biasing network. First, we can pick the value for a voltage potential V_{C1} at the collector of transistor Q_1. Second, we are free in our choice of the collector current through Q_1. Since I_{B2} should not be affected by current fluctuations in I_{C1}, we choose I_{C1} such that $I_{C1} = 10I_{B2}$ (i.e., $I_{C1} = 1\text{ mA}$). Then the current I_1 through resistor R_{C1} is composed of collector current I_{C1} and two base currents I_{B1} and I_{B2}; that is,

$$I_1 = I_{C1} + I_{B1} + I_{B2} = I_{C1}(1 + \beta_1^{-1}) + I_{C2}/\beta_2 = 1.11\text{ mA}$$

Assuming $V_{C1} = 3\text{ V}$, we find

$$R_{B2} = \frac{V_{C1} - V_{BE2}}{I_{B2}} = 22\text{ k}\Omega \text{ and } R_{C1} = \frac{V_{CC} - V_{C1}}{I_1} = 1.8\text{ k}\Omega$$

Another degree of freedom is the choice of voltage V_{E1} at the emitter terminal of the transistor Q_1. Setting V_{E1} to 1 V, we find

$$R_{B1} = \frac{V_{C1} - V_{BE1} - V_{E1}}{I_{B1}} = 120\text{ k}\Omega$$

and

$$R_{E1} = \frac{V_{E1}}{I_{C1} - I_{B1}} = 1.11\text{ k}\Omega$$

Finally, the collector resistor R_{C2} is determined to be

$$R_{C2} = (V_{CC} - V_{CE2})/I_{C2} = 200\ \Omega$$

Although active biasing offers a number of performance advantages over passive networks, certain disadvantages also arise:

specifically, additional circuit board space, possible layout complications, and added power requirements.

Another active biasing network for a BJT in common-emitter configuration is shown in Figure 8-34. Here diodes D_1 and D_2 provide a fixed reference for the voltage drop across the base-emitter junctions of both transistors. Resistor R_1 is used to adjust the biasing current to the base of transistor Q_1 and R_2 limits the range of this adjustment. Ideally, for temperature compensation, transistor Q_1 and one of the diodes should remain at ambient temperature, whereas the second diode should be placed on the same heat-sink as RF transistor Q_2.

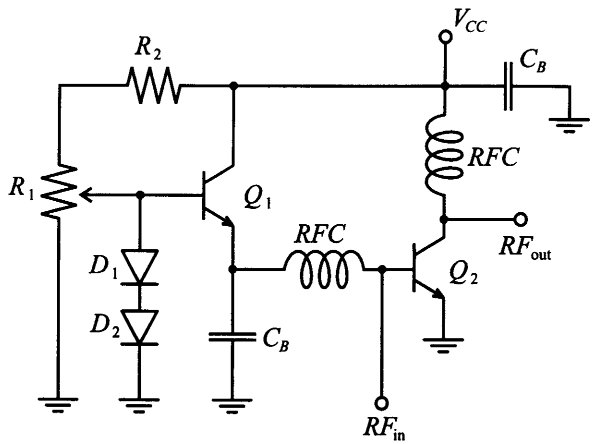

Figure 8-34 Active biasing network containing low-frequency transistor and two diodes.

As a final remark, it is important to point out that in all biasing networks the operational conditions (common-base, common-emitter, or common-collector) of the transistor at RF frequencies are entirely independent of the DC configuration. For instance, we can take an active biasing network, shown in Figure 8-33, and modify it for common-base RF operation, as seen in Figure 8-35.

At DC all blocking capacitors represent an open circuit and all RFCs behave like short circuits. Therefore, this biasing network can be redrawn as shown in Figure 8-36(a), indicating the common-emitter configuration. However, at RF frequency all blocking capacitors become short circuits and all RFCs behave like open circuits. This transforms the biasing network into a common-base mode, as depicted in Figure 8-36(b).

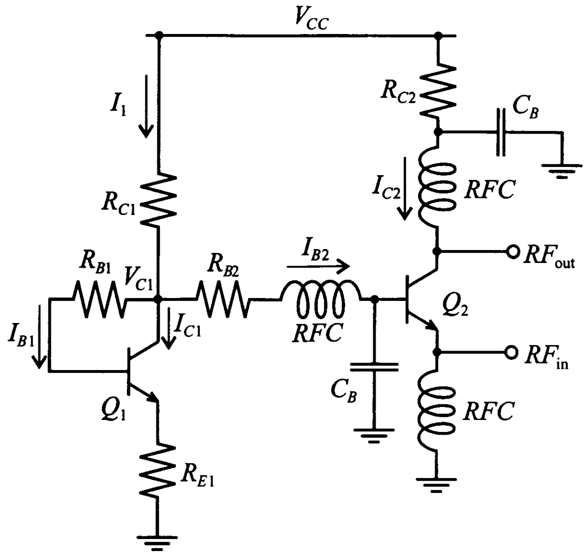

Figure 8-35 Modification of the active biasing network shown in Figure 8-33 for a common-base RF operation.

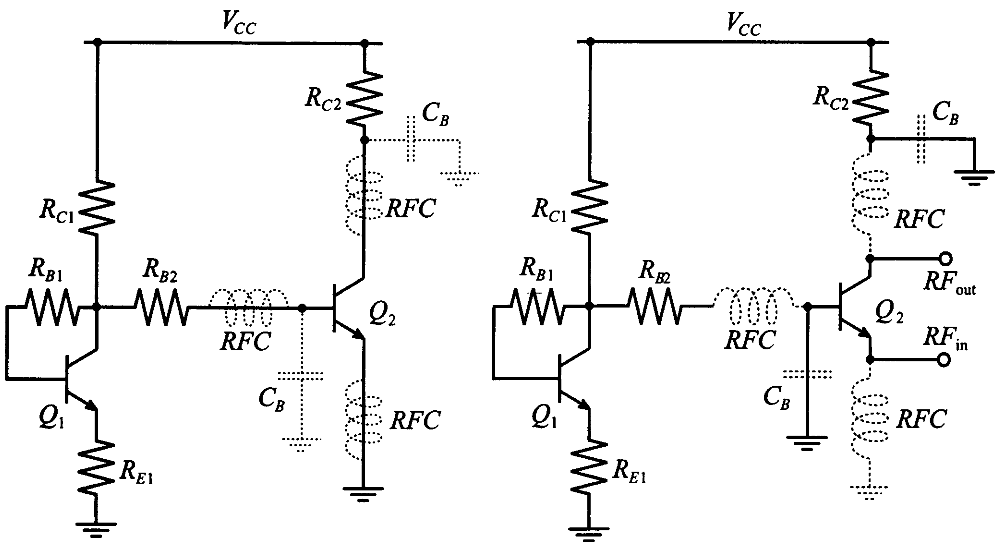

(a) DC equivalent circuit (b) RF equivalent circuit

Figure 8-36 DC and RF equivalent circuits for the active biasing network in Figure 8-35.

8.3.3 Field Effect Transistor Biasing Networks

The biasing networks for field effect transistors are in many ways very similar to the BJT networks covered in the previous section. One key distinction is that MESFET usually require a negative gate voltage as part of the bias conditions.

The most basic passive bipolar biasing network for FETs is shown in Figure 8-37.

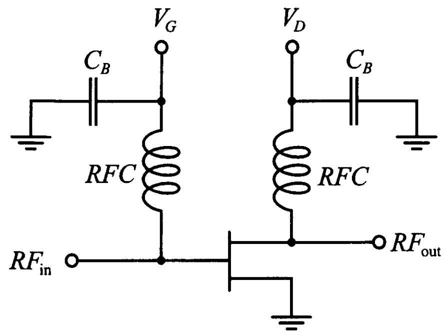

Figure 8-37 Bipolar passive biasing network for FETs.

The main disadvantage of such a network is the need of a bipolar power supply for $V_G < 0$ and $V_D > 0$. If such a bipolar power supply is unavailable one can resort to a strategy where instead of the gate, the source terminal of the transistor is biased. The gate in this case is grounded. Two examples of such networks are shown in Figure 8-38.

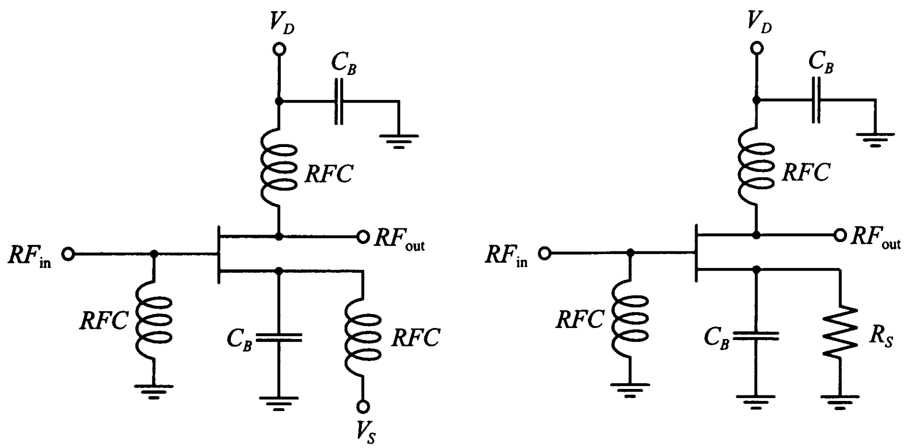

Figure 8-38 Unipolar passive biasing networks for FETs.

The temperature compensation of the FET biasing networks is typically accomplished through the use of thermistors.

8.4 Summary

The material covered in this chapter is geared toward providing an understanding of two key issues encountered in any RF/MW system: interfacing various components of different impedance values, and suitably biasing the active devices depending on their class of operation.

To ensure optimal power transfer between systems of different impedances, we investigate at first two-element L-type matching configurations. In the context of two-port network analysis, the conjugate complex matching requirement at the input and output ports results in optimal power transfer at a particular target frequency. The technique is simple and can be compared with the design of a bandpass or bandstop filter. Care must be exercised in selecting a suitable L-type network to avoid the forbidden regions for which a given load impedance cannot be matched to the desired input impedance. From the knowledge of the network transfer function, the loaded quality factor

$$Q_L = \frac{f_0}{BW}$$

and the simpler to compute nodal quality factor

$$Q_n = \frac{|X_S|}{R_S} = \frac{|B_P|}{G_P}$$

can be utilized as a measure to assess the frequency behavior of the matching networks. Unfortunately, L-type networks do not allow any flexibility in conditioning the frequency response and are therefore mostly used for narrow band RF designs. To affect the frequency behavior, a third element must be added, resulting in T- and Pi-type networks. With these configurations a certain nodal quality factor, and indirectly a desired bandwidth, can be implemented.

While the lumped element design is appropriate at low frequencies, distributed transmission line elements must be employed when the frequency extends into the GHz range. The hybrid configurations of using series connected transmission line elements and shunt connected capacitors are very attractive for prototyping since the location and value of the capacitors can easily be varied. If the capacitors are replaced by open- and short-circuit transmission lines, one arrives at the single- and double-stub matching networks.

Depending on the application (for instance, linear small signal or nonlinear large signal amplification), various classes of transistor amplifiers are identified. The classification is done by computing the RF to supply power ratio, known as efficiency:

$$\eta = \frac{P_{RF}}{P_S}100\%$$

which can be expressed in terms of the conduction angle Θ_0 quantifying the amount of load current flow through the relation

$$\eta = \frac{\Theta_0 - \sin\Theta_0}{2[\Theta_0\cos(\Theta_0/2) - 2\sin(\Theta_0/2)]}$$

For instance, Class A offers the highest linearity at the expense of the lowest efficiency of 50%, whereas Class B compromises linearity but improves efficiency to 78.5%.

Once the class of operation is identified, a biasing network is chosen to set the appropriate quiescent point of the transistor. Passive biasing networks are normally easy to implement. However, they are not as flexible as biasing networks involving active devices. The biasing not only sets the DC operating conditions but must also ensure isolation of the RF signal through the use of RFCs and blocking capacitors.

Further Reading

W. A. Davis, *Microwave Semiconductor Circuit Design,* Van Nostrand Reinhold Company, New York, 1984.

N. Dye and H. Granberg, *Radio Frequency Transistors: Principles and Practical Applications,* Butterworth-Heinemann, 1993.

G. Gonzalez, *Microwave Transistor Amplifiers: Analysis and Design,* Prentice Hall, Upper Saddle River, NJ, 1997.

P. Horowitz and W. Hill, *The Art of Electronics,* Cambridge University Press, Cambridge, UK, 1993.

D. Pozar, *Microwave Engineering,* John Wiley & Sons, New York, 1998.

P. Rizzi, *Microwave Engineering: Passive Circuits,* Prentice Hall, Englewood Cliffs, NJ, 1988.

Problems

8.1 Obtain the "forbidden" regions for the two-element matching networks shown in Figures 8-1(c)–(f). Assume that the load is matched to the normalized input impedance (i.e., $z_{in} = 1$).

8.2 Use the analytical approach and design a two-component matching network that matches the $Z_L = (100 + j20)\Omega$ load impedance to a given $Z_S = (10 + j25)\Omega$ source, at the frequency of $f_0 = 960$ MHz.

8.3 Develop a two-component matching network for a $Z_L = (30 - j40)\Omega$ load and a 50 Ω source. How many network topologies exist that can be used? Find the values of the components if a perfect match is desired at $f_0 = 450$ MHz.

8.4 Repeat Problem 8.3 for a $Z_L = (40 + j10)\Omega$ load and a matching frequency of $f_0 = 1.2$ GHz.

8.5 Measurements indicate that the source impedance in Problem 8.3 is not purely resistive but has a parasitic inductance of $L_S = 2$ nH. Recompute the values for the matching network components that take into account the presence of L_S.

8.6 A load $Z_L = (20 + j10)\Omega$ consisting of a series R-L combination is to be matched to a 50 Ω microstrip line at $f_0 = 800$ MHz. Design two two-element matching networks and specify the values of their components. Plot a frequency response for both networks and find the corresponding bandwidths.

8.7 In Example 8-5 a T-network is discussed that matches a load impedance of $Z_L = (60 - j30)\Omega$ to an input impedance of $Z_{\text{in}} = (10 + j20)\Omega$ at 1 GHz, under the constraint that Q_n does not exceed the factor of 3. Step-by-step go through this design and identify each point in the Smith Chart in terms of its impedance or admittance values. Verify the final results shown in Figure 8-16.

8.8 Go through Example 8-6 and find each point in the Smith Chart shown in Figure 8-17 and verify the final network components depicted in Figure 8-18.

8.9 Repeat the Pi-type matching network design in Example 8-6 for a nodal quality factor of $Q_n = 2.5$. Plot $Z_{\text{in}}(f)$ for this Q_n value and compare it against the $Q_n = 2$ design in Example 8-6. As frequency range, choose $1\text{ GHz} < f < 4\text{ GHz}$.

8.10 Design two T-type matching networks that transform a $Z_L = 100\ \Omega$ load to an $Z_{\text{in}} = (20 - j40)\Omega$ input impedance at a nodal quality factor of $Q_n = 4$. The matching should be achieved at $f_0 = 600$ MHz.

8.11 Design two Pi-type matching networks for the same conditions as in Problem 8.10.

8.12 To achieve matching conditions for a specified Q_n, the circuit designer has to use more than two or three elements in the matching network. Using a graphical approach, design a multisection matching network that transforms $Z_L = 10\ \Omega$ into $Z_S = 250\ \Omega$ at $f_0 = 500$ MHz while maintaining a nodal quality factor of $Q_n = 1$. The multisection matching network should consist of a series of two-element sections each of which is a "series inductor, shunt capacitor" combination [see Figure 8-1(h)].

8.13 For an increased frequency of $f_0 = 1$ GHz it was decided that the network designed in Problem 8.12 should be replaced by a combined matching network shown in Figure 8-19. Determine the total number of capacitors and transmission line sections necessary to achieve matching and find the values of all components in the network.

8.14 Using the design from Example 8-7, find the length and width of each transmission line if an FR-4 substrate with dielectric constant of $\varepsilon_r = 4.6$ and height of $h = 25$ mil is used. Find the maximum deviation of the input impedance of the matching network if the capacitor that is used in the circuit has a $\pm 10\%$ tolerance and the automatic component placement equipment has a ± 2 mil precision (i.e., the capacitor can be placed within ± 2 mil of the intended position).

8.15 In Example 8-7 it is argued that open-circuit stubs can be replaced by short-circuit ones if the length is increased by a quarter wavelength. Matching is achieved only for a single frequency, and over a broader frequency range the network response can significantly differ from the target impedance values. Design a single-stub matching network that transforms a $Z_L = (80 + j20)\Omega$ load impedance into a $Z_{\text{in}} = (30 - j10)\Omega$ input impedance. Compare the frequency response over the $\pm 0.8 f_0$ frequency range for two different realizations of the matching network: open-circuit stub, and using an equivalent short-circuit stub. Assume that the matching frequency is $f_0 = 1$ GHz and the load is a series combination of resistance and inductance.

8.16 Using the matching network shown in Figure 8-23(b), find the stub length l_S, the characteristic line impedance Z_{0L}, and the transmission line length l_L such that the $Z_L = (80 - j40)\Omega$ load impedance is matched to 50 Ω source. Assume that the characteristic impedance of the stub is $Z_{0S} = 50\ \Omega$.

8.17 For a double-stub tuner shown in Figure 8-26 with parameters $l_1 = \lambda/8$, $l_2 = 5\lambda/8$, and $l_3 = 3\lambda/8$, determine to which end of the tuner a $Z_L = (20 - j20)\Omega$ load has to be connected and find the length of the short-circuited stubs such that the load is matched to a 50 Ω line. Assume that all stubs and transmission lines in the tuner have a 50 Ω characteristic impedance.

8.18 Discuss a circuit configuration that replaces in the previous problem the stub tuners with varactor diodes in series with inductors. Choose the appropriate inductances if the varactor diodes can change their capacitances in the range from 1 pF to 6 pF. For a frequency of 1.5 GHz discuss the tuning capabilities in terms of possible load impedance variations.

8.19 An ideal amplifier has a transfer function given by the equation

$$V_{\text{out}} = \begin{cases} 30(V_{\text{in}} - V^*), & V_{\text{in}} \ge V^* \\ 0, & V_{\text{in}} < V^* \end{cases}$$

where $V^* = 60$ mV. Find the quiescent point (V_Q and I_Q) and the corresponding maximum efficiency such that the amplifier is operated in the AB class and has conductance angle of $\Theta_0 = 270°$. Assume that the input signal is a sinusoidal voltage wave of 100 mV amplitude.

8.20 Find the component values for a low-GHz range biasing network for a BJT with bypassed emitter resistor R_3, as shown below:

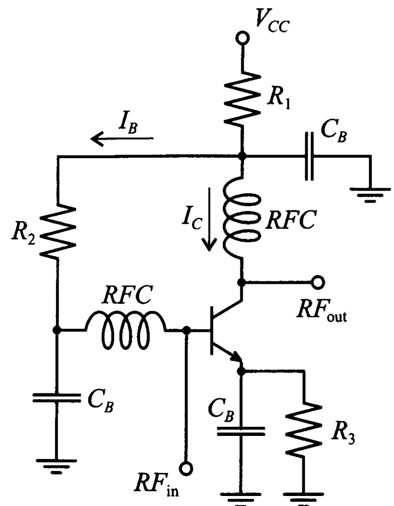

Assume that the power supply voltage is $V_{CC} = 12$ V and the transistor has the following parameters: $I_C = 20$ mA, $V_{CE} = 5$ V, $\beta = 125$, and $V_{BE} = 0.75$ V.

8.21 For stability purposes a feedback resistor $R_F = 1\ \text{k}\Omega$ has been added between base and collector of the transistor in the biasing network shown in Figure 8-32(b). Compute the values of all resistors in the biasing network if the following biasing conditions must be satisfied: supply voltage of $V_{CC} = 5$ V, collector current of $I_C = 10$ mA, and collector-emitter voltage of $V_{CE} = 3$ V. Assume that the transistor has a $\beta = 100$ and a $V_{BE} = 0.8$ V.

8.22 Design a biasing network (shown in the following figure) for $I_{C2} = 10$ mA, $V_{CE2} = 3$ V, and $V_{CC} = 5$ V. Assume that $\beta_1 = 150$, $\beta_2 = 80$, and both transistors have $V_{BE} = 0.7$ V.

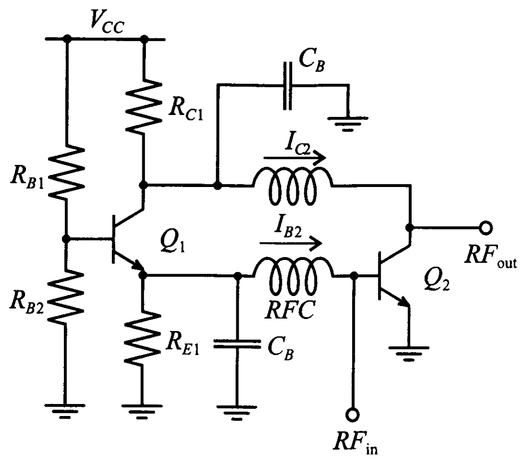

8.23 Redraw the active biasing network shown in Figure 8-34 for a common-base and a common-collector operating mode, respectively.

8.24 For the passive FET biasing network shown in Figure 8-38, find the value of the source resistance R_S if $V_{GS} = -4$ V, $V_{DS} = 10$ V, and the drain current is given to be $I_D = 50$ mA.